Construction and Characterization of 3rd Generation *Saccharomyces cerevisiae* Strains for PHB production from Xylose

Degree Project in Masters Biotechnology Programme

Pálína Haraldsdóttir

LUND UNIVERSITY
FACULTY OF ENGINEERING
DEPARTMENT OF CHEMISTRY
DIVISION OF APPLIED MICROBIOLOGY
2018

Supervisor: Lisa Wasserstrom
Examiner: Marie Gorwa-Grauslund

Abstract

Poly-3-D-hydroxybutyrate (PHB) is a biopolymer naturally produced by a range of bacterial species. PHB production both from glucose and xylose has also been enabled by engineering the robust baker's yeast *Saccharomyces cerevisiae*, however yields remain low. In the present study, additional modifications were carried out in *S. cerevisiae* strains already expressing functional enzymatic pathways for PHB production from xylose. The first approach was to improve the efficiency of acetyl-CoA conversion to acetoacetyl-CoA in the PHB pathway by introducing enzymes possessing lower K_m for acetyl-CoA than the original expressed enzyme from *Cupriavidus necator*. Two distinct acetyl-CoA acetyltransferases were introduced, Acat1 from *Rattus norvegicus* and Erg10p from yeast using the CRISPR-Cas9 system; however no improvement in PHB production was obtained. The second approach was to increase the acetaldehyde pool so that the introduced heterologous acetylating acetaldehyde dehydrogenases (EutE) encoded by *eutE* would enhance the flux from acetaldehyde towards acetyl-CoA in one step using NAD^+, which should increase PHB production, when combined with deletion of the main acetaldehyde dehydrogenase (*ALD6)* gene. Obtained results showed no PHB production in any strains expressing the EutE and therefore it was assumed that EutE was catalysing the reaction in the reverse direction resulting in increased acetaldehyde, which led to further investigations of the enzyme involving activity and overall functionality. Deletion of the *eutE* gene was also carried out in (EutE carrying) non-PHB producing strains to see if the PHB production would be restored. The *eutE* was also re-integrated in PHB producing strains. However in both cases no PHB was produced. These results indicated that the EutE gene integration was inactivating PHB production since removal of *eutE* did not restore PHB production. Therefore, the negative effect of EutE might be at the genetic level on either one or several of the PHB genes *phaA*, *phaB* or *phaC*.

Popular Science Summary

Over the past years, concerns have increased worldwide regarding hazardous compounds, such as water- and air pollutants and waste disposal being spread to the environment. Solutions towards sustainability involve the replacement of non-renewable resources by renewable ones for the generation of bio-based and biodegradable materials. The microorganism *Saccharomyces cerevisiae*, also known as baker´s yeast, has been well studied and is commonly used for the production of such compounds. *S. cerevisiae* is very efficient for the utilization of 6-carbon sugars (also called "hexose" sugars) such as glucose as carbon source but in industrial applications it is preferable to use cheap and non-edible renewable feedstock for the production of biofuels and other chemicals. However non-edible biomass, such as wood or agricultural waste, often contain a large fraction of 5-carbon sugars (*aka* pentoses), notably xylose that cannot be naturally assimilated by *S. cerevisiae* so this yeast has been genetically engineered to enable xylose utilization, notably for producing the so-called 2nd generation bioethanol. Nowadays, *S. cerevisiae* is being foreseen as a putative platform organism for the generation of biodegradable plastic precursors from biomass as there is a strong will to reduce the production of petroleum-based plastics. Among bioplastics, the biopolymer poly-3-hydroxybutyrate (PHB) is a promising substitute for non-renewable polymers since it can be completely degraded under both anaerobic and aerobic conditions by means of various microorganisms. In this study, *S. cerevisiae* that already was genetically modified to produce PHB from xylose was further engineered to improve PHB levels. The strategy consisted in increasing, inside the cells, the pool of a precursor of PHB called acetyl-CoA. This was done by modifying the levels of some enzymes as well as adding more efficient enzymes. There was no improvement in PHB production; instead the study indicated that one of the introduced gene negatively impacted the correct function of some of the PHB genes.

Preface

Previous work and investigations had already been carried out in other studies which accompanied my researches during this study. The urgent need for alternatives embracing a sustainable future motivated me to keep pursuing this challenge and continue with further investigations.

Firstly, I want to thank my family, boyfriend and friends, which I am so grateful to have, for their unconditional support and understanding throughout my studies. I also want to thank my supervisor for the support and guidance during my project, as well as my examiner and everybody at the Applied Microbiology division for their help, advisement and overall assistance.

Table of content

Abbreviations

PHB: Poly-3-D-hydroxybutyrate
ACT: Acetyl-CoA acetyltransferase
AAR: Acetoacetyl-CoA reductase
PHS: Polyhydroxyalkanoate synthase
EutE: Acetylating acetaldehyde dehydrogenase
ALD: Acetaldehyde dehydrogenase
ADH: Alcohol dehydrogenase
Acat1: Acetyl-CoA acetyltransferase from *Rattus norvegicus*
Erg10p: Acetyl-CoA acetyltransferase from yeast
HPLC: High-Performance liquid chromatography
PCR: Polymerase chain reaction
OD: Optical density
CDW: Cell dry weight
CRISPR: Clustered regularly interspaced short palindromic repeats
gRNA: Guide RNA

1. Introduction

Environmental concerns have risen as the population is constantly increasing and problems like waste disposal, air- and water pollution etc. is taking a toll on Mother Earth. It is clear that alternatives are needed to sustain the environment for future generations. For a sustainable future, various alternatives have to be explored regarding provision of bio-based bulk chemicals from renewable feedstock. In that context biotechnology offers extended opportunities and possibilities with the help of living organism, and notably yeast.

1.1 Project background

Yeast as biocatalyst

The yeast *Saccharomyces cerevisiae* is a well studied eukaryote that is frequently used for industrial purposes since it is an excellent industrial fermentation organism due to its tolerance to low pH and high efficiency of fermenting sugars (Moysés *et al.* 2016). *S. cerevisiae* is known for its utilization of hexose sugars but it cannot naturally metabolize the pentose sugar xylose. However, since materials from renewable feedstock are often rich in xylose, large efforts have been invested in the last 20 years to also enable efficient xylose utilization in this yeast (Moysés *et al*, 2016; Hou *et al.* 2017).

Some bacteria metabolize xylose using a xylose isomerase (XI) that converts xylose directly to xylulose (Jeffries 1983) while in yeasts such as *Scheffersomyces stipites*, a two-step oxido-reductase process including the two enzymes xylose reductase (XR) and xylitol dehydrogenase (XDH) is more prevalent (du Preez and Prior 1985). Both avenues result in the conversion of xylulose to xylulose-5-P by the means of xylulose kinase (XK) which can then enter the pentose phosphate pathway (PPP) and glycolysis (Wang and Schneider 1980). Introducing the XR/XDH pathway into *S. cerevisiae* has enabled yeast to utilize xylose. As the xylulose-5-P enters the Pentose phosphate pathway (PPP), chemicals such as ethanol, acetate, glycerol etc. can be produced, as illustrated in Figure 1 (Moysés *et al.* 2016).

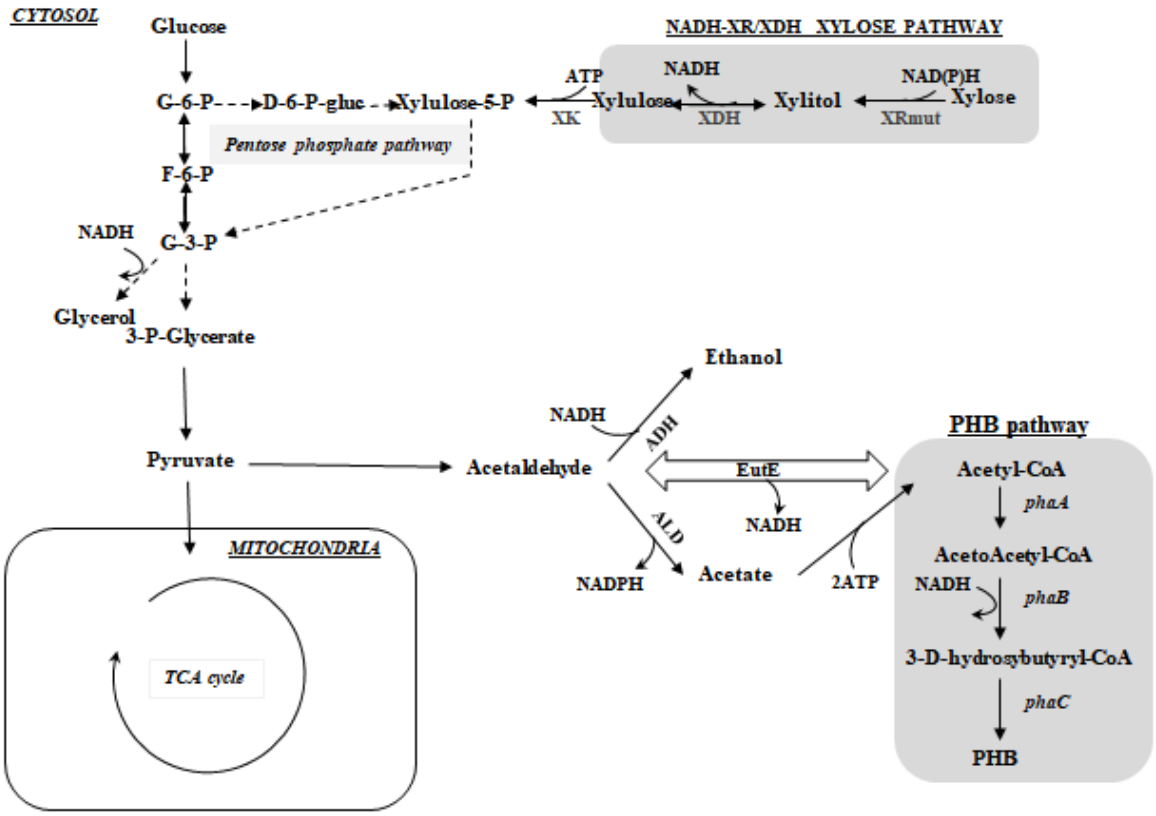

Figure 1. A simplified schematic overview of the metabolism of recombinant *S. cerevisiae* strains that contain the XR_{mut}/XDH and PHB pathways where the mutant XR enzyme has been engineered for increased affinity for NADH (de las Heras 2017). The figure also includes the integrated EutE enzyme.

Bioplastics

Petroleum-based plastics are being used worldwide every day but strategies are currently being developed for substitution by greener alternatives. Bioplastics can be produced from renewable biomass resources, such as starch and cellulose. Bioplastics produce less greenhouse gases than the petroleum-based ones; however since the demand is so high, strategies for more efficient production on a large-scale are needed (Gironi and Piemonte 2011). Not all bioplastics are biodegradable though so the biodegradable biopolymers polyhydroxyalkanoates (PHAs) have been of great interest considering that they possess properties approaching those of synthetic polymers. PHAs can be completely degraded under both anaerobic and aerobic conditions by means of various microorganisms. The most common type of PHAs is poly-3-hydroxybutyrate (PHB) that can be naturally produced by diverse bacterial species and used as a storage molecule under certain nutrient limiting conditions. For large scale productions, *Escherichia coli* has been engineered to produce PHB but, as the process is expensive and subjected to recurrent phage infections, alternatives are needed (Sandström *et.al.* 2015). Since *S. cerevisiae* is commonly used as a cell factory platform, it is a promising candidate for PHB production (Sandström *et.al.* 2015; Lee 1996).

The PHB pathway is associated with three enzymes: an acetyl-CoA acetyltransferase (ACT) encoded by *phaA*, an acetoacetyl-CoA reductase (AAR) encoded by *phaB* and finally a

polyhydroxyalkanoate synthase (PHS) encoded by *phaC* (Carlson and Srienc 2006). *phaA*, *phaB* and *phaC* from *Cupriavidus necator* have successfully been introduced into *S. cerevisiae* and PHB production was demonstrated (Sandström *et al*. 2015; Carlson and Srienc 2006). Nonetheless, PHB titres from engineered *S. cerevisiae* remain low and further optimisation is needed.

Several alternative routes have been studied to enhance PHB production from xylose in *S. cerevisiae* strains carrying the xylose pathway as well as the PHB pathway. De las Heras (2016-a) demonstrated that increased amounts of PHB were reached from xylose in *S. cerevisiae* strains containing XR_{mut}/XDH after introduction of NADH-dependent AAR from *A. vinosum* instead of the bacterial NADPH-dependant AAR from *C. necator* (cf. Figure 1). Since the biomass synthesis is NADPH-dependent, the introduced NADH-dependant AAR did not compete for NADPH, leading to more PHB production (de las Heras 2016-a; Sandström *et al.* 2015). For further optimization of the PHB pathway, several heterologous acetyl-CoA acetyltransferase enzymes with higher affinity for acetyl-CoA than ACT encoded by *phaA* have been studied to improve the conversion from Acetyl-CoA to acetoacetyl-CoA (Yun 2015). Another strategy is to increase the flux towards acetyl-CoA. In *S. cerevisiae* acetyl-CoA is synthesised from pyruvate in several steps as Figure 2 illustrates involving following enzymes: pyruvate decarboxylase, acetaldehyde dehydrogenase (ALD) and acetyl-CoA synthetase (Saint-Prix *et al*. 2004).

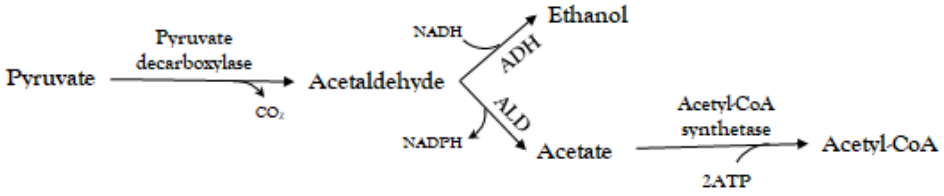

Figure 2. A schematic overview of the conversion of pyruvate to acetyl-CoA in *Saccharomyces cerevisiae*.

During the conversion from acetaldehyde to acetyl-CoA, ethanol and acetate are formed catalysed by alcohol dehydrogenase (ADH) and acetaldehyde dehydrogenase (ALD) respectively. In a study aiming at boosting biomass formation from ethanol, it was shown that by introducing the heterologous acetylating acetaldehyde dehydrogenase (EutE) encoded by the *eutE* gene from *E. coli* in *S. cerevisiae,* acetyl-CoA could be synthesised directly from acetaldehyde in one step using NAD^+ as a cofactor (Fig. 1) (Kozak *et al.* 2014; Medina *et al.* 2010).

By introducing EutE in PHB-producing *S. cerevisiae,* a new, ATP-independent route for production of acetyl-CoA could be provided to enhance the flux from acetaldehyde to acetyl-CoA. However, since the EutE reaction is reversible, deletion of the main alcohol dehydrogenase, *ADH1*, and the main acetaldehyde dehydrogenase, *ALD6* (Fig. 2), might be needed.

1.2 Aim of the study

The aim of the study was to construct and characterize a 3rd generation of *S. cerevisiae* strains for PHB production from xylose. The PHB-producing *S. cerevisiae* strains were engineered to enhance the acetyl-CoA formation as well as improve the efficiency of PHB production. Modifications were mostly performed using the CRISPR-Cas9 gene editing method: Clustered Regularly Interspaced Short Palindromic Repeats (CRISPR) and CRISPR-associated (Cas) systems can be found in bacteria where they are involved in the adaptive immune system where foreign DNA is used to eventually destroy any matching DNA sequences (Gupta and Musunuru 2014). Cas9 is a RNA guided endonuclease which cleaves the native double stranded DNA at a specific site where a donor DNA can then be integrated. The Cas9 recognises the PAM sequence and cleaves the DNA three nucleotides upstream (Fig. 3) (Hsu, Lander and Zhang 2014; Jessop-Fabre *et al.* 2016).

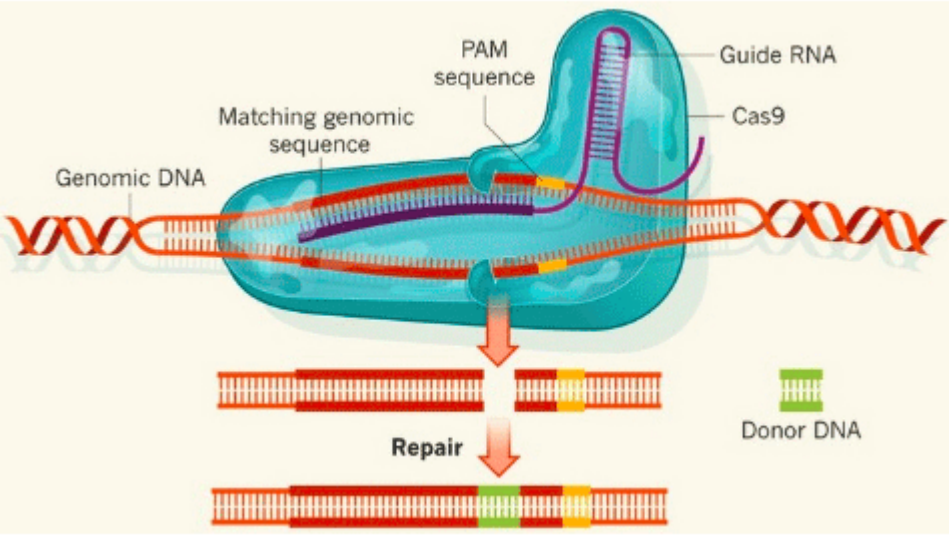

Figure 3. A simplified overview of the CRISPR-Cas9 system (http://www.sinobiological.com/crispr-cas9-knockin-cell-lines-genome-editing.html).

The CRISPR-Cas9 system has been adapted for genetic engineering of eukaryotic cells which can lead to some great possibilities and leverage in the near future. Many advantages of using the CRISPR-Cas9 system compared to other genome editing tools have been demonstrated such as being relatively easy and quick procedure as well as being able to target multiple genes at the same time etc. (Young, Aitken and Ikawa 2015).

2. Materials and methods

2.1 Strains, media and culture conditions

E. coli strain NEB5α containing desired plasmids were grown at 37 °C in Luria-Bertani (LB) medium containing 10 g/l tryptone, 5 g/l yeast extract, 5 g/l NaCl, pH 7.5 supplemented with 50 mg/l ampicillin. Yeast strains were grown at 30 °C and 180 rpm in an orbital shaker under non-selective conditions in Yeast Peptone Dextrose (YPD) medium containing 10 g/l yeast extract, 20 g/l peptone and 20 g/l glucose. Competent cells were prepared and the subsequent transformation was performed according to the high-efficiency LiAc protocol with the small modification that 10 % DMSO was added prior to the heat shock at 42 °C for 20 minutes (Gietz and Schiestl 2007). When yeast cells were transformed using the CRISPR-Cas9 system, cells were propagated in YPD containing 200 mg/l geneticin (G418) and transformants were selected on YPD media supplemented with 200 mg/l G418 and 100 mg/l nourseothricin. When yeast cells were transformed using the amdSYM cassette as selection marker, colonies were selected on synthetic media containing acetamide (SM-Ac) according to Solis-Escalante *et al*. (2013).

In Table 1, plasmids used in present study are listed as well as relevant genotypes.

Table 1. Plasmids used in current study.

Plasmid name	Relevant genotype	Reference
pCfB2903	XI-2-MarkerFree	Jessop-Fabre *et al*. (2016)
pCfB3034	X-3-MarkerFree	Jessop-Fabre *et al*. (2016)
pCfB3039	XII-2-MarkerFree	Jessop-Fabre *et al*. (2016)
pCFB3050	gRNA_XII-5	Jessop-Fabre *et al*. (2016)
pCfB3051	gRNA_X-3_XI-2_XII-2	Jessop-Fabre *et al*. (2016)
LWA42	pCfB2903+*TEFp-ERG10-ADH1t*	Perruca Foncillas (2018)
LWA43	pCfB3034+*TEFp-ERG10-ADH1t*	Perruca Foncillas (2018)
LWA44	pCfB3039+*TEFp-ERG10-ADH1t*	Perruca Foncillas (2018)
pUGamdSYM	(A.g.)*TEF1p-amdS-(A.g.)TEFt*	Solis-Escalante *et al*. (2013)
pUC57-EutE	*TEF1*p-*eutE-CPS1*t	de las Heras (2017)

2.2 Yeast strain engineering

In Table 2, an overview of used and constructed *S. cerevisiae* strains included in the current study are listed as well as relevant genotypes and features.

Table 2. *S. cerevisiae* strains used in current study.

Strain name	Relevant genotype	Relevant features	Reference
TMB4425	CEN.PK2-1C; Δ*gre3*;*his3::pPGK1-XKS1-PGK1t;HIS3;tal1:: pPGK1-TAL1-PGK1t; tkl1:: pPGK1-TKL1-PGK1t;rki1:: pPGK1-RKI1-PGK1t; rpe1:: pPGK1-RPE1-PGK1t; pTEF1-phaA-TEF1t; pTPI1-AvphaB-TPI1t; pGMP1-phaC1-GMP1t*	XR/XDH, PHB-NADH	de las Heras *et al*., (2016-a)
TMB4425Cas9	TMB4425; *pTEF1p-Cas9-CYC1t*_kanMX	XR/XDH, PHB-NADH, Cas9	de las Heras *et al*., (2016-b)
TMB4495Cas9	TMB4425Cas9; XII-5::*eutE*	XR/XDH, PHB, EutE	de las Heras (2017)
TMB4498Cas9	TMB4495Cas9; Δ*adh1*	XR/XDH, PHB, EutE, Δ*adh1*	de las Heras (2017)
TMB4800	TMB4425Cas9; X-3::ΔN30acat1opt; XI-2::ΔN30acat1opt; XII-2::ΔN30acat1opt	XR/XDH, PHB, 3xΔN30acat1opt	Perruca Foncillas (2018)
TMB4801	TMB4495Cas9; X-3::ΔN30acat1opt; XI-2::ΔN30acat1opt; XII-2::ΔN30acat1opt	XR/XDH, PHB, EutE, 3xΔN30acat1opt	Perruca Foncillas (2018)
TMB4802	TMB4498 Cas9; X-3::ΔN30acat1opt; XI-2::ΔN30acat1opt; XII-2::ΔN30acat1opt	XR/XDH, PHB, EutE, Δ*adh1*, 3xΔN30acat1opt	Perruca Foncillas (2018)
TMB4803	TMB4800; Δ*ald6::amdSYM*	XR/XDH, PHB, 3xΔN30acat1opt, Δ*ald6*	Perruca Foncillas (2018)
TMB4804	TMB4801; Δ*ald6::amdSYM*	XR/XDH, PHB, EutE, 3xΔN30acat1opt, Δ*ald6*	Perruca Foncillas (2018)
TMB4805	TMB4802; Δ*ald6::amdSYM*	XR/XDH, PHB, EutE, Δ*adh1*, 3xΔN30acat1opt, Δ*ald6*	Perruca Foncillas (2018)
TMB4809	TMB4425Cas9; X-3::*ERG10*; XI-2:: *ERG10*; XII-2:: *ERG10*	XR/XDH, PHB, 3xErg10p	This study
TMB4810	TMB4495Cas9; X-3:: *ERG10*; XI-2::*ERG10*; XII-2:: *ERG10*	XR/XDH, PHB, EutE, 3xErg10p	This study

TMB4811	TMB4498Cas9; X-3:: *ERG10*; XI-2:: *ERG10*; XII-2:: *ERG10*	XR/XDH, PHB, EutE, Δ*adh1*, 3xErg10p	This study and Perruca Foncillas (2018)
TMB4812	TMB4809; Δ*ald6::amdSYM*	XR/XDH, PHB, 3xErg10p, Δ*ald6*	This study
TMB4813	TMB4810; Δ*ald6::amdSYM*	XR/XDH, PHB, EutE, 3xErg10p, Δ*ald6*	This study
TMB4495Δ*eutE*	TMB4425Cas9; XII-5::Δ*eutE::amdSYM*	XR/XDH, PHB, Δ*eutE*	This study
TMB4498Δ*eutE*	TMB4495Cas9; Δ*adh1;* XII-5::Δ*eutE::amdSYM*	XR/XDH, PHB, EutE, Δ*adh1*	This study
TMB4800+EutE	TMB4425Cas9; X-3::ΔN30acat1opt; XI-2::ΔN30acat1opt; XII-2::ΔN30acat1opt; XII-5::*eutE*	XR/XDH, PHB, 3xΔN30acat1opt, EutE	This study
TMB4803+EutE	TMB4800; Δ*ald6::amdSYM;* XII-5::*eutE*	XR/XDH, PHB, 3xΔN30acat1opt, Δ*ald6*, EutE	This study
TMB4809+EutE	TMB4425Cas9; X-3::*ERG10*; XI-2:: *ERG10*; XII-2:: *ERG10;* XII-5::*eutE*	XR/XDH, PHB, 3xErg10p, EutE	This study

Once the yeast cells had been transformed, verification was carried out on several selected clones using colony-PCR followed by gel electrophoresis. Each clone/colony was picked up from the transformation plates with a loop in the sterile hood and a small amount of cells were transferred to an Eppendorf containing 15 µl of 0.02 M NaOH. To disrupt the cells the samples were boiled in a heating block for 10 min and quickly centrifuged for ~30 sec at 13.200 rpm. 1 µl of the supernatant was then transferred to a PCR tube and a PCR reaction mix added to a final volume of 20 µl. In Table 3, 4 and 5, PCR reaction mixes, amplification target, primers and PCR product sizes are listed for each integration and deletion.

Three copies of the overexpression cassette containing *TEF1p-ERG10-ADH1t* had previously been introduced into *S. cerevisiae* strains TMB4425, TMB4495 and TMB4498 using the CRISPR-Cas9 system (Perruca Foncillas 2018). However, since correct integration had not been verified, PCR verification was performed in the current study. Several clones for each transformed strain was picked and DNA was extracted as described above. Three different PCR reactions were prepared where each primer set contained one unique primer annealing to a specific intergenic region on chromosome X-3, XI-2 or XII-2 in combination with one primer annealing in the *ERG10* cassette resulting in PCR1, 2 and 3, respectively, as shown in Table 3. Only strain TMB4498 could be verified to carry all three copies of *ERG10* and therefore transformation of TMB4425 and TMB4495 had to be re-done. In order to integrate three copies of the *ERG10* overexpression cassette, plasmids LWA42-44 were extracted from the *E. coli* NEB5α glycerol stocks using the GeneJET plasmid miniprep kit (Thermo Fischer Scientific,

Waltham, MA, USA). The concentration of each purified plasmid was measured at 260 nm using BioDrop DUO UV/VIS Spectophotometer. 1500 ng of each plasmid was cleaved with Fastdigest *Smi*I (Thermo Fischer Scientific, Waltham, MA, USA) to release the cassette and correct cleaving was verified by agarose gel electrophoresis. The linearized plasmid were transformed into strains TMB4425Cas9 and TMB4495Cas9 together with the gRNA plasmid pCfB3051 which should cleave in a specific intergenic regions in chromosome X-3, XI-2 and XII-2 and thereby facilitating triple integration (Jessop-Fabre *et al*., 2016).

Table 3. Verification of correct integration in 3x*ERG10* constructed yeast strains. PCR reaction mix, amplification targets, primer sets and PCR product sizes are listed.

PCR	Amplification target	Forward primer (Primers no. and sequence)	Reverse primer (Primers no. and sequence)	PCR Size
#1	XI-2::*ERG10*	7_kanMXUP (5'-GCACGTCAAGACTGTCAAGG-3')	324_XI-2 (5'-ACTGGGAACAGAAATCGACC-3')	816 bp
#2	X3::*ERG10*	7_kanMXUP (5'-GCACGTCAAGACTGTCAAGG-3')	323_X3 (5'-CCTGAAGGAAAAAGAGGTGG-3')	625 bp
#3	XII-2::*ERG10*	7_kanMXUP (5'-GCACGTCAAGACTGTCAAGG-3')	322_XII-2 (5'-CGGTTGACCATAGTATTCACC')-3')	914 bp

ALD6 gene deletion was then carried out in verified 3x*ERG10* strains, TMB4809, TMB4810 and TMB4811 using the amdSYM cassette. pUG-amdSYM marker was used and primers listed in Table 4 were used to design the *ALD6* deletion cassette. Both the forward and reverse primers contained a 50 bp sequence homologous to the upstream and downstream of *ALD6*.

Table 4. Verification of correct integration of the amdSYM marker to disrupt the *ALD6* gene. PCR reaction mix, amplification targets, primer sets and PCR product sizes are listed.

PCR	Amplification target	Forward primer* (Primers no. and sequence)	Reverse primer* (Primers no. and sequence)	PCR size
#1	5' integration Δ*ald6::amdSYM*	9_G1_ALD6 (5'-CATCAAAACACCGTTCGAGG-3')	6_amdSYMup (5'-cgaggagccgtaatttttgc-3')	493 bp
#2	3' integration Δ*ald6::amdSYM*	5_amdSYMdown (5'-ccagatgcgaagttaagtgc-3')	10_G4_ALD6 (5'-AGCAGTTGTTGTACACTAGC-3')	443 bp
#3	*ALD6*	11_I1_ALD6 (5'-	12_I1_ALD6 (5'-	581 bp

		GAACTTCACCAC CTTAGAGC-3')	TAGCACCTTGGAAGTTAGCC -3')	
-	Δ*ald6*::amdSYM cassette	1_S1_ALD6 (5'-AAAACATCAAGA AACATCTTTAACA TACACAAACACA TACTATCAGAAT Atgaagcttcgtacgctgca g-3')	2_S2_ALD6 (5'-TATATGAAAGTATTTTGTGT ATATGACGGAAAGAAATGC AGGTTGGTACAacgactcactatag ggagac-3')	2536 bp

*Uppercase sequences represent the genomic regions of *S. cerevisiae* while lowercase sequences represent the annealing regions of the amdSYM cassette.

For Δ*eutE*, pUG-amdSYM was used as a marker and primer 341f and 342r were used to amplify the *eutE* deletion cassette. The forward primer contained a 49 bp sequence homologous to the end of the promoter in the *eutE* cassette and a 20 bp sequence homologous to the S1 annealing region on the amdSYM cassette. The reverse primer contained 50 bp homology to the start of the *eutE* terminator and 22 bp homology to the S2 annealing region. Clones were verified with colony-PCR prepared using three different primer sets as listed in Table 5.

eutE integration in chromosome XII-5 was then carried out in strains TMB4800, TMB4803 and TMB4809 using CRISPR-Cas9 system. To integrate the *eutE* cassette, plasmid pUC57-EutE+amp was extracted from *E. coli* NEB5α glycerol stocks using the GeneJET plasmid miniprep kit (Thermo Fischer Scientific, Waltham, MA, USA). The concentration of the purified plasmid was measured at 260 nm using BioDrop DUO UV/VIS Spectophotometer. The plasmid was transformed into strains strains TMB4800, TMB4803 and TMB4809 together with the gRNA plasmid pCfB3050 which should cleave in a specific intergenic regions in chromosome XII-5 and thereby facilitating integration (Jessop-Fabre *et al.*, 2016).

Table 5. Verification of correct integration of the Δ*eutE::amdSYM* deletion cassette and subsequent removal of the *eutE* ORF. in constructed yeast strains. PCR reaction mix, amplification targets, primer sets and PCR product sizes are listed.

PCR	Amplification target	Forward primer (Primers no. and sequence)	Reverse primer (Primers no. and sequence)	PCR size
#1	5' integration XII-5::Δ*eutE::amdSYM*	343_XII-5 up (5'-GAGTCAAGTTAGGTCA TCCC-3')	6_amdSYMup (5'-cgaggagccgtaatttttgc -3')	451 bp
#2	3' integration XII-5::Δ*eutE::amdSYM*	5_amdSYM down (5'-ccagatgcgaagttaagtgc-3')	261 (5'-AATAGCAAACGGC CAGTAGC-3')	426 bp
#3	XII-5::*eutE*	343_XII-5 up (5'-GAGTCAAGTTAGGTCA TCCC-3')	Seq_EutE (5'-GCAATTGTTGTGC TTGTTCAGC-3')	1471 bp

*Uppercase sequences represent the genomic regions of *S. cerevisiae* wile lowercase sequences represent the annealing regions of the amdSYM cassette.

2.3 Enzymatic Assay

Enzyme activity assays were performed for further verification of the constructed strains. Three different enzymatic assays were performed in technical duplicates: AAR activity assay (encoded by *phaB* or alternative genes to *phaB*), ALD activity assay and EutE activity assay (Table 6). All enzyme activities were measured at 340 nm for 10 minutes at 30 °C using a Multiskan Ascent microtiter plate reader (Thermo Electro Corporation, Finland) where the cell extract for each strain was prepared and measured in two concentrations, undiluted and 5x diluted in H_2O. For each enzymatic assay, the specific activity was calculated for each dilution and expressed as µmol substrate conversion per minute per mg protein (µmol/min mg protein).

Table 6. An overview of different enzymatic assays performed on constructed yeast strains.

AAR activity assay	Aldp activity assay	EutE activity assay
TMB4425	TMB4425	TMB4425
TMB4495	TMB4494	TMB4495
TMB4498	TMB4497	TMB4498
TMB4801	TMB4804	TMB4801
TMB4804	TMB4805	TMB4804
TMB4805	TMB4812	TMB4805
TMB4809	TMB4813	TMB4809
TMB4810		TMB4810
TMB4811		TMB4811
TMB4812		TMB4813
TMB4813		TMB4803+EutE clone #E
TMB4803+EutE clone #E		TMB4498ΔEutE clone #B
TMB4498ΔEutE clone #B		TMB4498ΔEutE clone #D
TMB4498ΔEutE clone #D		

Selected strains were cultivated in 5 ml YPD glucose (50 g/l) medium in 50 ml Falcon tubes in a shaking incubator (30 °C, 180 rpm) overnight. Cells were collected by centrifugation (4000 x g), the cell pellet was washed once in 1 ml sterile water and the cell pellet was resuspended in either 250 µl, 100 µl or 75 µl (depending on the pellet size) of the Yeast Protein Extraction Reagent (YPER) (Pierce, Rockford, IL, USA) and protein were extracted by incubating at room temperature for 20 minutes. Total protein concentration was determined using the Bradford protein assay kit (Sigma-Aldrich) and Bovine serum albumin (Sigma-Aldrich) as standard. 250 µl of Bradford solution was added to a 96-well microtiter plate as well as 5 µl of sample/standard/blank. All samples were diluted 5 times. After mixing, the plate was incubated for 10 minutes at room temperature after which the absorbance was measured at 595 nm using a Multiskan Ascent microtiter plate reader (Thermo Electro Corporation, Finland). The protein concentration in all samples was then calculated using the standard curve.

2.3.1 AAR activity assay

AAR activity was measured by monitoring the oxidation of NADH at 340 nm in a 200 µl reaction mixture containing 200 mM MOPS, pH 7.0, 100 mM 2-mercaptoethanol, 4 mM acetoacetyl-CoA, 4 mM NADH and 10 µl of cell extract. Before adding the NADH to the reaction, the background was monitored. The assay was performed as previously described by de las Heras *et al.,* (2016-a).

2.3.2 ALD activity assay

ALD activity was measured by monitoring the reduction of $NADP^+$ at 340 nm in a 200 µl reaction mixture containing 1 M potassium phosphate pH 8.0, 150 mM pyrazole, 20 mM DTT 1 M $MgCl_2$, 20 mM $NADP^+$, 50 mM acetaldehyde and 10 µl of cell extract. Before adding the substrate (acetaldehyde), the background was monitored. The assay was performed as previously described by de las Heras *et al.*, (2016-b).

2.3.3 EutE activity assay

EutE activity was measured by monitoring the reduction of NAD^+ at 340 nm in a 200 µl reaction mixture containing 500 mM CHES, pH 9.5, 4 mM coenzyme A, 20 mM NAD^+, 1M acetaldehyde, 10 µl of cell extract. Before adding the substrate (acetaldehyde), the background was monitored. The assay was performed as previously described by Kozak *et al.* (2014).

2.4 Aerobic cultivation in shake-flask

Prior cultivations, verified transformed yeast cells were pre-cultivated in 50 ml falcon tubes containing 5 ml 2x yeast nitrogen base - (YNB; 6.7 g/L YNB without amino acids; Becton–Dickinson, NJ, USA) supplemented with 50 g L^{-1} xylose and grown for approximately 18 h in a shaking incubator at 30 °C and 180 rpm. Cultivations were then prepared in 1 L shake flasks containing 100 ml of 2x YNB supplemented with 50 g L^{-1} xylose and inoculated to a starting OD_{620} of 0.05. Optical density was measured using an Ultrospec 2100 Pro spectrophotometer (Amersham Biosciences Corp., USA). Samples (2 ml) were taken and cells were spun down for 5 min at 6100 RCF. The supernatant was transferred to new Eppendorf tubes (for metabolite analysis) and stored at -20 °C while the remaining pellet was washed twice in 1 ml of sterile MQ-H_2O and centrifuged at 6100 RCF for 5 min between each washing step. The washed pellet was stored at -20 °C and later used for PHB extraction.

2.5 Cultivation under reduced aerobic conditions

Cultivations under reduced aerobic conditions was carried out with strain TMB4805 using 250 ml shake flasks without baffles, magnetic beads for stirring and a waterbath set to 30 °C for temperature control. The strain was pre-cultivated in 5 ml YNB with 2 % glucose in a 50 ml Falcon tube and incubated overnight at 30 °C and shaking at 180 rpm. Four 250 ml shake flasks were prepared with different volume of 2x YNB + 5 % xylose: 62.5 ml (25%), 125 ml (50%), 187.5 ml (75%) and 225 ml (90%) where the medium was inoculated to a starting OD of 0.1. Indicated in brackets is the volume percentage of media in relation to the total shake flask volume of 250 ml. The OD was measured at 10 time points: 0 h, 48 h, 96 h, 120 h, 144 h, 168

h, 186 h, 234 h, and 258 h while PHB and metabolite samples were collected at 7 time points: 0 h, 96 h, 121 h, 144 h, 168 h,188 h and 258 h.

2.6 PHB quantification

The PHB quantification and extraction was performed as described by Law and Slepecky (1961). For PHB extraction, the cell pellet was resuspended in 500 µl of 95-97 % sulfuric acid (Sigma-Aldrich), vortexed carefully and put into a heat block at 95 °C for 1 h with the lids open. The samples were then left to cool down to room temperature and vortexed. The samples were then diluted 10x in deionized water, vortexed and centrifuged for 1 min at maximum speed. A second 2x dilution was done in deionized water and centrifuged for 1 min at maximum speed, resulting in a final 20x diluted sample. Samples were analysed with HPLC as described below where the crotonic acid is the compound of interest.

2.7 Metabolite analysis and cell dry weight determination

The supernatant containing the metabolites were analysed using the HPLC Waters systems (Milford, USA) equipped with an Aminex HPX-87H column (Bio-Rad, Richmond, USA) operating at 60 °C with a mobile phase of 5 mM H_2SO_4 and a flow rate of 0.6 ml min^{-1}. Xylose, xylitol, glycerol, acetate and ethanol were detected and quantified using a RID-10A refractive index detector (Shimadzu, Japan) and an external calibration curve of the components. PHB was detected using the same conditions as for the analysis of metabolites and quantified by comparing to an external calibration curve of crotonic acid.

The cell dry weight (CDW) was determined in duplicate at the end of the cultivation (160 h) using pre-weighed and dried nitrocellulose filters with 0.45 µm pore size (ø 47mm) (PALL, USA). Cell suspension was filtered with vacuum pump and washed three times. The filters were dried and weighed after excess moisture had been eliminated in a desiccator at room temperature. Biomass was correlated to OD_{620} by a single point calibration from the final measuring time point.

2.7.1 Analytical problems involving xylose concentration in samples

During the HPLC analysis a problem regarding the initial xylose values occurred. Overall the xylose concentration in the initial time points, where the xylose concentration was the highest, varied a lot between strains either increasing or decreasing even if it was clear that the strains had not started to grow. Approximately the first 2 to 4 sampling points gave inconsistent results in several cases and therefore new dilutions were made of these samples and analysed again with HPLC (a Waters system equipped with an Aminex HPX-87H column). Similar results occurred in the second run which led to third run with another Waters system that contained the same hydrogen column. After the third run, the values turned out to have the same problem as with the C5LT HPLC machine. Similar observations had been made by other lab members and it could be concluded that that samples containing xylose in high concentration should not be frozen, but only stored on ice until analysed. Due to these problematic xylose values occurring in several cultivations, the starting values which showed reasonable xylose concentration were used from the same cultivation instead of the wrong ones.

3. Results

3.1 Overexpression of different acetyl-CoA acetyltransferases with increased affinity for acetyl-CoA to improve the flux towards PHB from xylose.

3.1.1 Aerobic cultivation of PHB strains overexpressing *Acat1* from *R. norvegicus* or the endogenous *ERG10*

Previous studies have shown that introduction of EutE in the PHB producing strains TMB4425 (XR/XDH, PHB) and TMB4496 (XR/XDH, PHB, Δ*adh1*) completely abolished PHB formation (de las Heras, 2017). It was therefore hypothesised that the EutE reaction was going in the reverse direction, converting acetyl-CoA to acetaldehyde, thereby removing the substrate for the first enzyme in the PHB pathway, the acetyl-CoA acetyltransferase PhaA. In the present study, two different PhaA with higher affinity for acetyl-CoA were introduced and evaluated to enable more efficient competition with EutE for the available acetyl-CoA and drive the EutE reaction in the desired direction, from acetaldehyde to acetyl-CoA.

Three copies of the PhaA homolog, Acat1 from *R. norvegicus*, without the mitochondrial targeting sequence to allow cytosolic localisation (ΔN30acat1opt), had previously been introduced into TMB4425 (XR/XDH, PHB), TMB4495 (XR/XDH, PHB, EutE) and TMB4498 (XR/XDH, PHB, EutE, Δ*adh1*) generating strains TMB4800 (XR/XDH, PHB, Acat1), TMB4801 (XR/XDH, PHB, EutE, Acat1) and TMB4802 (XR/XDH, PHB, EutE, Δ*adh1*, Acat1), respectively. The aim was to improve the conversion of acetyl-CoA to acetoacetyl-CoA since Acat1 has lower K_m for acetyl-CoA than the currently used PhaA enzyme from *C. necator* (Middleton 1974). The strains had previously been cultivated under aerobic conditions in YNB containing 50 g/l xylose and the results showed slightly increased PHB titer (0.27 ± 0.05 g PHB/l) in TMB4800 compared to TMB4425 (0.25 ± 0.04 g PHB/l), respectively, (Perruca Foncillas 2018) as can be seen in Figure 4. No PHB was produced in TMB4495, TMB4498, TMB4801 and TMB4802 containing the *eutE* inserted gene. When comparing the xylose consumption, TMB4801 consumed 62.8 ± 6.0 % of the xylose which was the highest consumption observed in this cultivation followed by TMB4425 which consumed 56.2 ± 6.4 %.

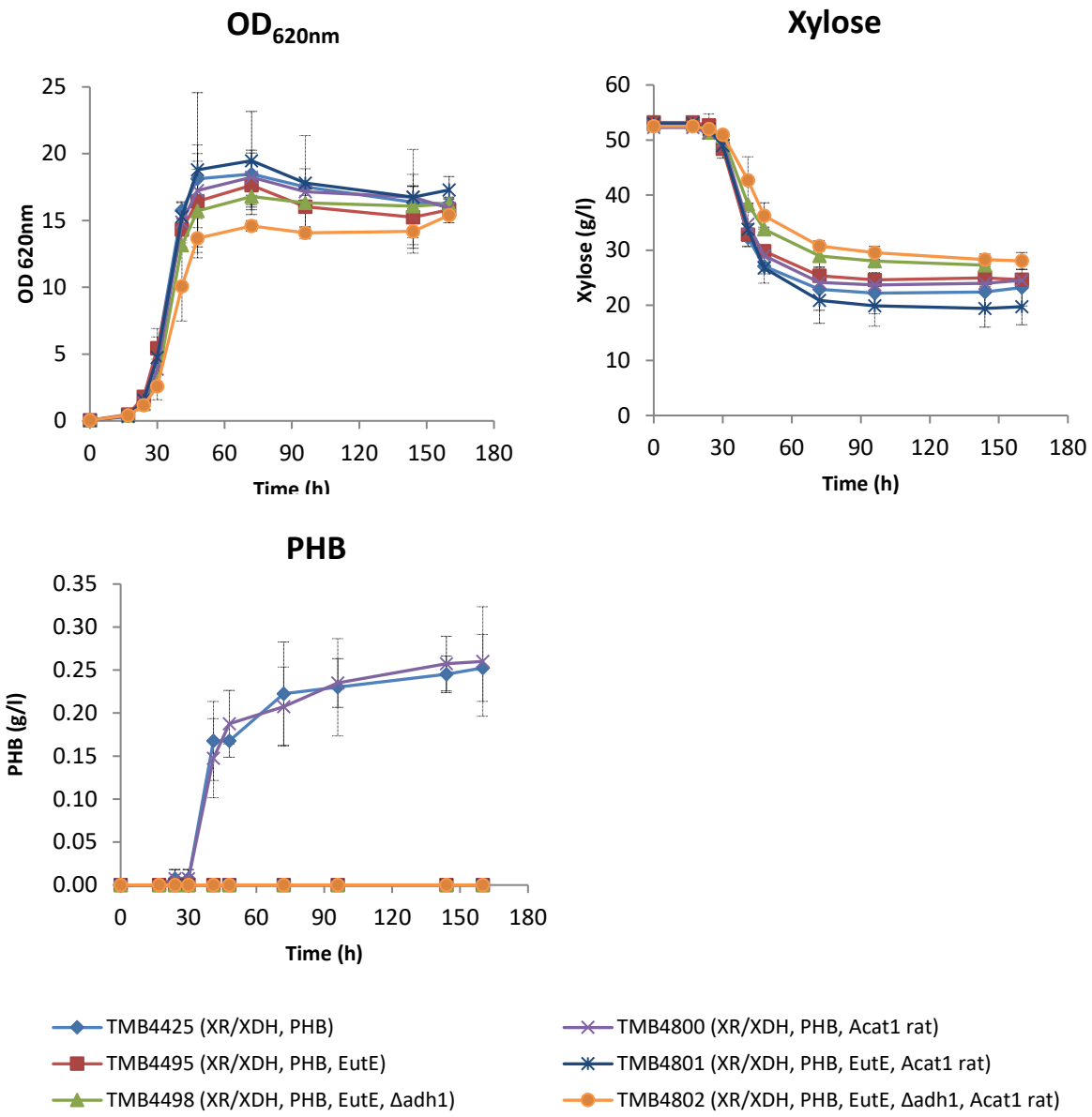

Figure 4. Growth, xylose consumption and PHB production in strains TMB4425, TMB4495, TMB4498, TMB4800, TMB4801 and TMB4802 grown in shake-flasks under aerobic conditions. The cultivations were done in another study and shown here as a comparison (Perruca Foncillas 2018). The values represent the average of two biological replicates and the error bars represent the standard deviation.

Due to the lack of PHB production in strains TMB4801 and TMB4802, containing Acat1, there was a possibility that the mitochondrial Acat1 from *R. norvegicus* was not functionally expressed in the cytosol of the yeast cells. To achieve cytosolic expression, the first 30 amino acids containing the mitochondrial tag had been removed, which might have affected the protein folding and thereby the function of the enzyme. Therefore the endogenous gene, *ERG10* coding for an acetyl-CoA acetyltransferase involved in ergosterol biosynthesis in yeast, (Hiser, Basson and Rine 1994) was introduced instead. Erg10p catalyses the formation of acetoacetyl-CoA from acetyl-CoA during ergosterol biosynthesis, which is the same reaction catalysed by PhaA in the PHB pathway. The advantage with Erg10p is that it has a lower K_m for acetyl CoA

(K_m=160 µM, accession number: P41338) than PhaA from *C. necator* (K_m=360 µM, accession number P14611) originally expressed in the PHB pathway. The aim was to see if PHB production would increase after overexpression of *ERG10* in the previously generated strains TMB4425 (XR/XDH, PHB), TMB4495 (XR/XDH, PHB, EutE) and TMB4498 (XR/XDH, PHB, EutE, Δ*adh1*).

In a previous study (Perruca Foncillas 2018), three copies of constitutively expressed *ERG10* were introduced into TMB4425, TMB4495 and TMB4498 using the CRISPR-Cas9 system that allows triple integration in three different intergenic regions on chromosome X, XI and XII (Jessop-Fabre *et al.*, 2016). Correct integration at all the three loci had not been verified and was therefore carried out in this study. Three different PCR reactions were run (Fig. 5) that would only allow amplification if the *ERG10* cassette had been correctly integrated in locus XI-2 (PCR1), X3 (PCR2) and XII-2 (PCR3). For this purpose three primer sets were used resulting in different product sizes (Table 3). Three integrated copies of *ERG10* were detected in all three clones (A-C) of TMB4498. However the integration of only one copy of *ERG10* on chromosome XII-2 was confirmed for all clones in TMB4425. In TMB4495, 2 out of the 3 copies were confirmed (chromosome X3 and XII-2).

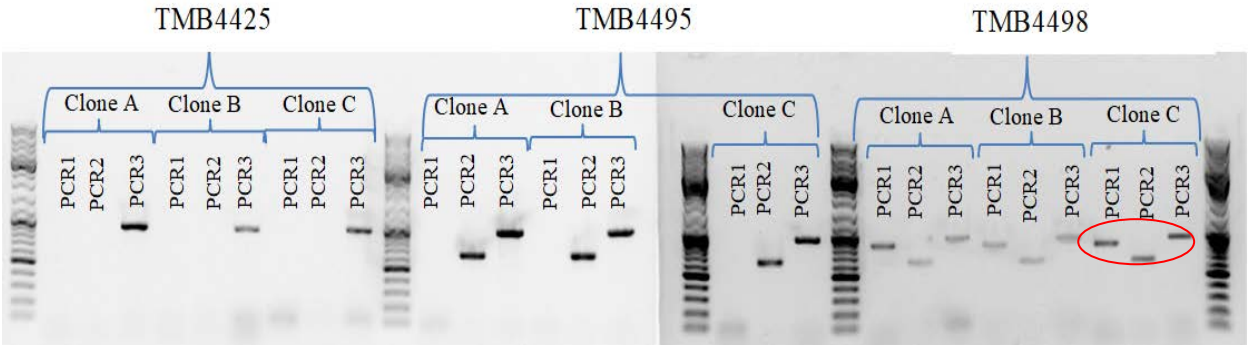

Figure 5. Verification of correct integration of three copies of *ERG10* in strains TMB4425, TMB4495 and TMB4498. For each yeast strain, three clones were chosen and three different primer sets were used to verify each copy in the right locus on the different chromosomes. PCR1 verifies integration on chromosome XI-2, PCR2 on chromosome X3 and PCR3 on chromosome XII-2. TMB4498 clone C with correct integration was saved as TMB4811 as indicated with a red cycle.

Due to failed integration of all three *ERG10* copies in TMB4425 and TMB4495, the two strains were constructed again in the current study using the CRISPR-Cas9 system as previously described (Perruca Foncillas 2018). Three clones from each transformed strain were selected and verified with colony-PCR using the same three PCR reactions as above, PCR1, PCR2 and PCR3. As can be seen in Figure 6, detection of all 3 copies could be confirmed in two clones of both TMB4425 and TMB4495 (marked with a red circle). Clone #C for all strains, as indicated with a red circle were saved as TMB4809 (TMB4425+*ERG10*), TMB4810 (TMB4495+*ERG10*) and TMB4811 (TMB4498+*ERG10).*

Figure 6. Verification of correct integration of three copies of *ERG10* in strains TMB4425 and TMB4495. For both strains, three clones were chosen and three different primer sets were used to verify each copy in the right locus on different chromosomes. PCR1 verifies integration on chromosome XI-2, PCR2 on chromosome X3 and PCR3 on chromosome XII-2. Correct verified clones are indicated with a red circle.

Verified clones (#C) expressing all three copies of the *ERG10* were cultivated in shake flasks under aerobic conditions in biological duplicates where OD_{620nm} was measured along with substrate consumption and production formation (Fig. 7). Yields were calculated for TMB4809, TMB4810 and TMB4811 and are listed in Appendix I (Table 9).

In Figure 7 below, growth, xylose consumption and PHB production for the reference strains (TMB4425, TMB4495 and TMB4498) and the overexpressing *ERG10* yeast strains can be seen. The values correspond to the average of the duplicates and the error bars correspond to the standard deviation. The results show that only TMB4809 was able to produce PHB while no PHB was observed in TMB4810 and TMB4811. The PHB titer for TMB4809 was 0.25 ± 0.04 g/l which was exactly the same as observed for TMB4425. The PHB yield was 8.40 ± 0.43 mg PHB/ g xylose for TMB4425 while 8.62 ± 1.14 mg PHB/ g xylose was observed for TMB4809. Interestingly, all strains overexpressing *ERG10* strains showed increased xylose consumption compared to the reference strains and the Acat1 overexpressing strains (Appendix I, Table 8 and 9). Overall, only the strains derived from TMB4425 (TMB4800 and TMB4809) were able to produce PHB while no PHB production was observed in strains derived from TMB4495 and TMB4498. Furthermore, when the PHB production was compared between the PHB producing strains, the average PHB titer for TMB4425 and TMB4809 was equivalent while the PHB titer for TMB4800 was 0.02 g/l higher. The results indicate that no relevant improvement in PHB production was observed in *Acat1* or *ERG10* expressing yeast strains. Therefore, further investigations were performed to evaluate that the PHB pathway was still functional and active.

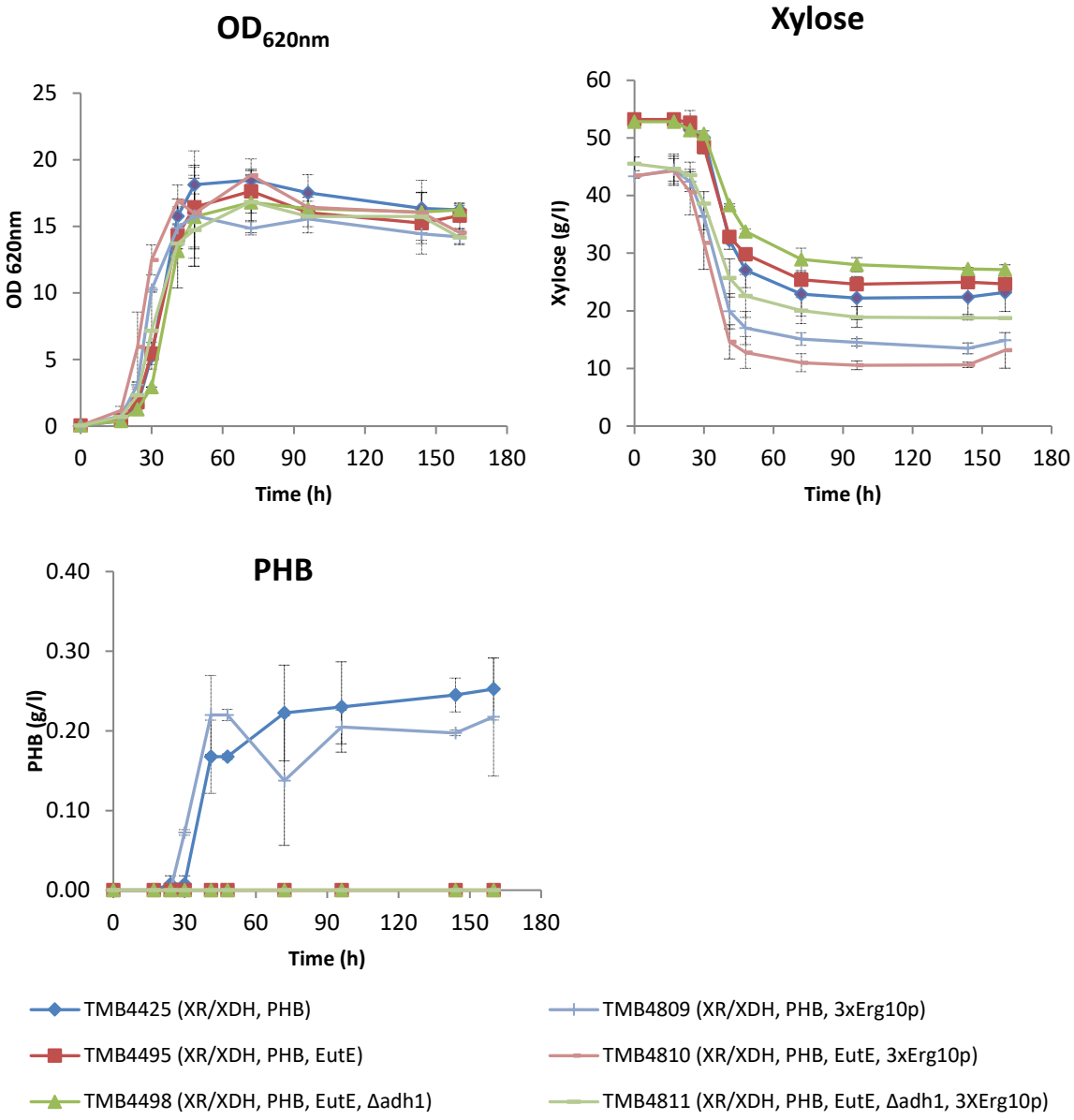

Figure 7. Growth, xylose consumption and PHB production of TMB4425, TMB4495, TMB4498, TMB4809, TMB4810 and TMB4811 grown in shake-flask under aerobic conditions. Strains TMB4425, TMB4495 and TMB4498 were cultivated in biological duplicates in another study (Perruca Foncillas 2018) but in current study, strains TMB4809, TMB4810 and TMB4811 were cultivated in biological duplicates. The values represent the average of the replicates and the error bars represent the standard deviation.

3.1.2 Acetoacetyl-CoA reductase (AAR) activity assay

Three enzymes are involved in the PHB pathway, ACT encoded by *phaA*, AAR encoded by *phaB* and PHS encoded by *phaC* and to evaluate if the pathway is functional, enzymatic activity assay can be performed. However, the enzyme activity of ACT, more specifically Acat1 and Erg10p which are encoded by alternative genes to *phaA*, would be an obvious choice to evaluate since the effect of the Acat1 and Erg10p on PHB production is being investigated in this study. Nonetheless, in another study (Perruca Foncillas 2018), ACT (Acat1 and Erg10p) activity measurements were performed but showed inconclusive results, which indicate that

different assay has to be applied for activity measurement of ACT. Due to time limitations in this study, alternative ACT activity assay was not further pursued. Instead, the activity of AAR was monitored to confirm that AAR (encoded by *phaB*) was being expressed and fully functional in the PHB pathway since no PHB production had been detected in strains generated from TMB4495 and TMB4498. Enzyme activity was performed at 340 nm on cell extract from strains expressing the *ERG10* and *Acat1*, by monitoring the oxidation of NADH to NAD^+ for 10 minutes at 30 °C as previously described. However, no activity was obtained from the measurements, not even in the positive control (PHB producing strains), which indicated that the assay was unreliable and not working as it should. Due to time limitations the assay could not be further optimized and therefore neither reliable results nor conclusions could be obtained.

3.2 Deletion of the aldehyde dehydrogenase 6 (*ALD6)* in *Acat1* and *ERG10* overexpressing PHB yeast strains to boost acetaldehyde to acetyl-CoA conversion by EutE

In this study it has been shown that strains expressing *eutE* are unable to produce PHB also after introduction of the two different PhaA with higher affinity for acetyl-CoA, namely Acat1 and Erg10p. Based on these findings we hypothesised that the direction of EutE towards acetyl-CoA might be improved by deletion of the main aldehyde dehydrogenase, *ALD6*, in yeast since such a strain should accumulate acetaldehyde. *ALD6* together with several other *ALD* genes, catalyses the conversion of acetaldehyde to acetate and in the case of Ald6p, $NADP^+$ is used as a coenzyme. In native yeast cells, *ALD6* deletion will result in decreased acetate formation and an increased flux towards ethanol due to the increased acetaldehyde pool (Luo *et al*., 2013) (Fig. 8).

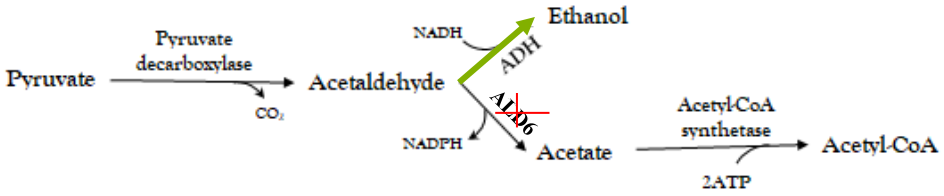

Figure 8. A schematic overview of the effects of *ALD6* gene deletion in native yeast cells resulting in increased acetaldehyde pool. The green arrow indicates increased flux towards ethanol and the red cross deletion of *ALD6*.

The *ALD6* gene had previously been deleted in strain carrying *Acat1* resulting in strains TMB4803 (XR/XDH, PHB, 3xAcat1rat Δ*ald6*), TMB4804 (XR/XDH, PHB, EutE, 3xAcat1rat, Δ*ald6*) and TMB4805 (XR/XDH, PHB, EutE, 3xAcat1rat, Δ*adh1* Δ*ald6*). In the present study, the *ALD6* gene was deleted in the Erg10p yeast strains TMB4809 (XR/XDH, PHB, 3xErg10p), TMB4810 (XR/XDH, PHB, EutE, 3xErg10p) and TMB4811 (XR/XDH, PHB, EutE, Δ*adh1*, 3xErg10p) using the amdSYM cassette (Fig. 9). Clones from the transformation plates were selected and verified with colony-PCR where three different PCR reactions were prepared each containing different primer sets. PCR1 and PCR2 represent correct integration of the amdSYM cassette upstream and downstream of the *ALD6* ORF,

respectively, which should result in a product size of 493 bp and 443 bp. PCR3 amplifies a region in the native *ALD6* gene and should therefore only give a product in clones still carrying the *ALD6* gene. Bands were detected for PCR1 and PCR2 in TMB4812 clones #C-1, #C-2 and #C-3 as well as TMB4813 clones #A-2, #C-1 and#C-3 corresponding to the correct deletion since no band could be seen for PCR3 in these clones. However, only bands for PCR3 were detected for TMB4811 derived clones, which indicates that the *ALD6* gene was still present. Correctly verified clones #C-3 of TMB4809 and #C-1 of TMB4810 carrying the *ALD6* deletions (indicated with a red circle in Fig. 9) were saved as TMB4812 and TMB4813, respectively.

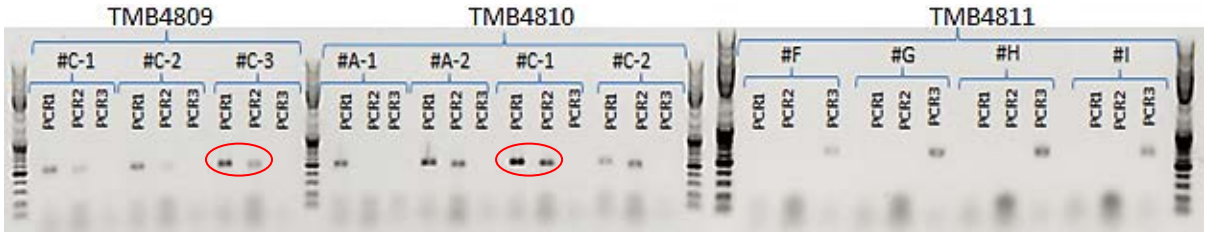

Figure 9. Verification of Δ*ald6* in TMB4809, TMB4810 and TMB4811 transformed strains generating TMB4812, TMB4813 and TMB4814. PCR1 and PCR2 represent correct integration of amdSYM and deletion of *ALD6* corresponding to 493 bp and 443 bp while PCR3 represent cells carrying the intact *ALD6* gene corresponding to 581 bp. Correct verified and saved clones are indicated with a red circle

3.2.1 Aerobic cultivation of *ALD6* deleted strains

The pre-constructed strains containing *Acat1* and Δ*ald6*: TMB4803 (XR/XDH, PHB, 3xAcat1rat Δ*ald6*), TMB4804 (XR/XDH, PHB, EutE, 3xAcat1rat, Δ*ald6*) and TMB4805 (XR/XDH, PHB, EutE, 3xAcat1rat, Δ*adh1* Δ*ald6*) were evaluated under aerobic conditions with respect to substrate consumption, metabolite formation and PHB production from xylose (Fig. 10 and 11). Cultivation of strains TMB4803 and TMB4804 had already been carried out in another study (Perruca Foncillas 2018) and here the cultivations were repeated to obtain a second replicate. Also the two newly generated strains TMB4812 and TMB4813 were cultivated. The strains were grown in shake-flasks under aerobic conditions following OD and metabolites over time (Fig. 10). The average values of the duplicates were used along with standard deviation. For comparison, the reference strains TMB4425 and TMB4495 were used. The yields calculated for the *ALD6* deleted strains are listed in Appendix I (Table 9). The xylose consumption in *ALD6* deleted strains, TMB4803, TMB4804, TMB4812 and TMB4813, was more efficient than in strains still carrying the *ALD6* gene. However, the high standard deviation calculated for TMB4803 indicated that a third replicate shall be carried out to get more reliable results.

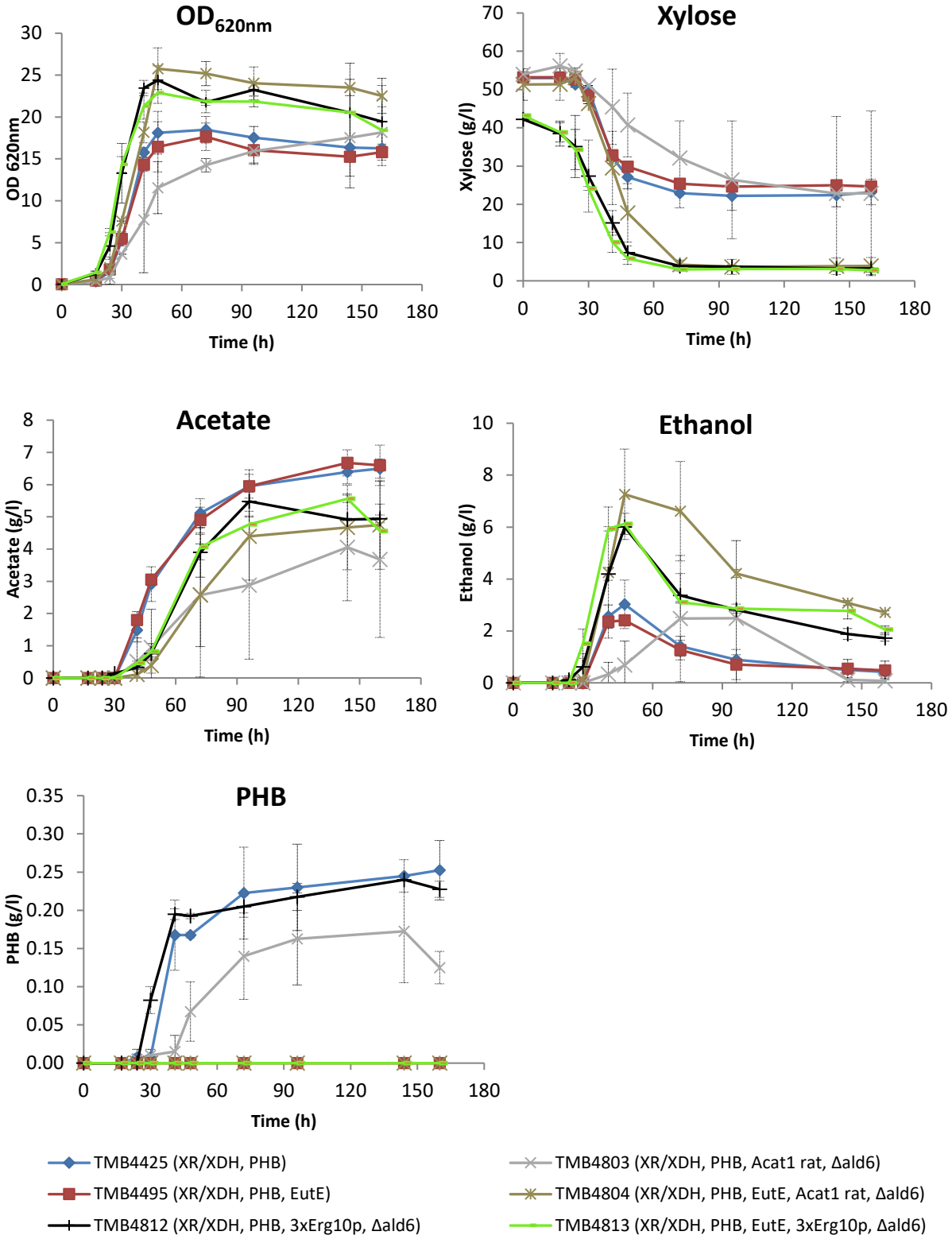

Figure 10. Substrate consumption and product formation of TMB44425, TMB4495, TMB4803, TMB4804, TMB4812 and TMB4813 grown in shake-flasks under aerobic condition. Strains TMB44425, TMB4495 were cultivated in biological duplicates and TMB4803 and TMB4804 in singlet in a previous study (Perruca Foncillas 2018) but in current study, the second replicate of TMB4803, TMB4804 was cultivated as well as TMB4812 and TMB4813 in biological duplicates. The values represent the average of the replicates and the error bars represent the standard deviation.

As Figure 10 indicates, the acetate formation decreased in the ALD6 deletion strains compared to TMB4425 and TMB4495, as expected; this also resulted in increased formation of ethanol as well as biomass. No improvement in PHB production was observed with *ALD6* deletion alone since the PHB titer for TMB4803 was 0.17 ± 0.07 g/l and 0.24 ± 0.00 g/l for TMB4812 while the PHB titer for TMB4425 was 0.25 ± 0.04 g/l. Since TMB4425, TMB4803 and TMB4812 do not express the EutE enzyme, no alternative route towards acetyl-CoA was present and therefore the pool of acetyl-CoA should decrease. Nonetheless the considerably higher xylose consumption in *ALD6* deleted strains explains the correlative PHB titer, especially for TMB4425 and TMB4812 where calculated yields confirm this (Appendix I, Table 8 and 9). However, *ALD6* deleted strains derived from TMB4495 carrying the *eutE* gene did still not produce any PHB. The *ALD6* had also been deleted in the *ADH1* deleted strain carrying the *Acat1*, generating TMB4805 (XR/XDH, PHB, EutE, Δ*adh1*, Acat1, Δ*ald6* however no growth under current conditions was observed (Perruca Foncillas 2018) and could therefore not be evaluated. The same strain but with *ERG10* could not be constructed in this study.

TMB4805 is very interesting since it carries two deletions Δ*adh1* and Δ*ald6*, which should lead to an accumulation of acetaldehyde and therefore provide enough substrate for EutE to drive that reaction in the desired direction, towards acetyl-CoA. But since the strain was not able to grow on xylose as the sole carbon source under aerobic conditions it was cultivated in YNB-glucose as well as in a combination of glucose and xylose. In Figure 11, the substrate consumption and the product formation can be seen depending on which medium the cells were cultivated in. Yields were also calculated and are listed in Appendix I (Table 10). No PHB was produced in TMB4805 neither when cultivated in glucose nor in combination of glucose and xylose. However as Figure 11 indicates, when TMB4805 was grown in a mixture of glucose and xylose, the cells were able to grow on xylose after all the glucose had been consumed. Due to this observation, cultivations were started on media containing only xylose but with varying aeration levels.

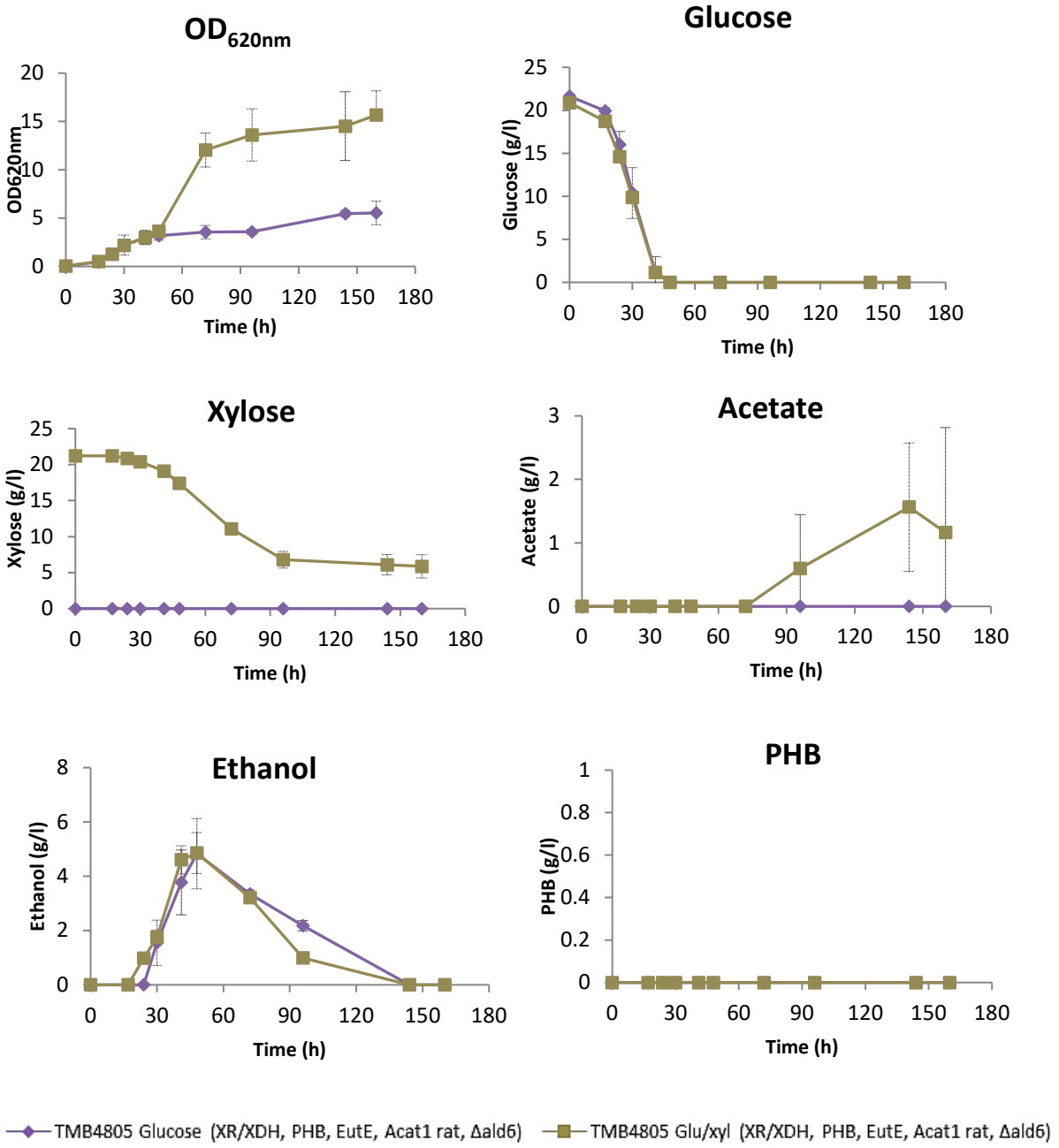

Figure 11. Substrate consumption and product formation of TMB4805 grown in a shake-flask under aerobic conditions. The strain was cultivated in biological duplicates in YNB supplemented with either 20 g L^{-1} glucose and or 20 g L^{-1} glucose and 20 g L^{-1} xylose. The values represent the average of the biological duplicates with standard deviation indicated with error bars.

3.2.2 Cultivation under reduced aeration

As the cultivations of TMB4805 in glucose/xylose media showed that the strain was able to grow on xylose, a set of experiments were designed to examine the impact of aeration in this strain. It was hypothesised that reduced aeration might be positive for xylose assimilation since more NADH will be available that can be used for ethanol and PHB formation. Four different shake flasks containing different levels of media (Fig. 12) were inoculated and incubated in a waterbath using a magnetic stirrer for mixing. As Figure 12 illustrates, TMB4805 was grown in 250 ml Erlenmeyer flasks containing different medium volumes; 62.5 ml, 125 ml, 187,5 ml

or 225 ml of YNB-xylose. Samples were collected as in previous cultivations during this study only on different time points. The OD was measured and metabolite samples were collected and analysed with HPLC. A summary of the data can be found in Appendix I (Table 10).

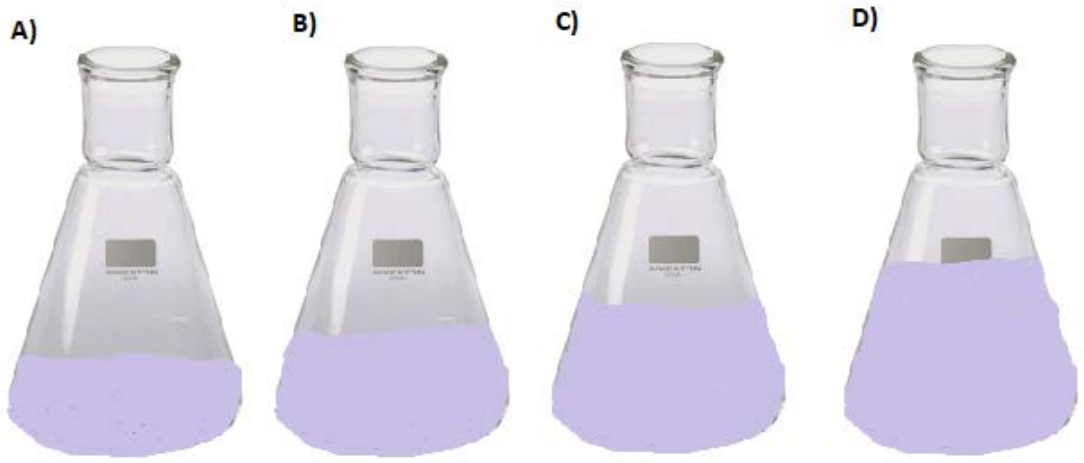

Figure 12. Schematic figure of reduced aeration cultivations of TMB4805 in 250 ml Erlenmeyer flasks containing different volumes of medium; A) 25 %: 62.5 ml, B) 50 %: 125 ml, C) 75 %: 187.5 ml, D) 90 %: 225 ml.

In Figure 13 the growth, xylose consumption and product formation can be seen. The strain was cultivated in singlet. TMB4805 was able to grow under all conditions, however, the best growth was seen in the flask with 25 % media indicating that oxygen was required for xylose assimilation. In the cultivations with 25 % and 50 % media, similar xylose consumption rates were observed, but only the culture with the most oxygen present (25% media) was able to respire the ethanol and produce additional biomass from it. When oxygenation was further decreased, the growth gradually decreased. Acetate was only formed at one time point in the 25 % media cultivation while ethanol formation increased and was highest, 14.58 g/l, in 50 % media culture. The biomass obtained in the 25 % culture was 6.53 g/l indicating that the cells could be using the acetyl-CoA to produce biomass since no PHB was produced. However with further decreased oxygenation, the biomass decrease could indicate that acetaldehyde was being accumulated causing cell death. Overall, even though the strain could grow on xylose, in contrast to what was previously reported (Perruca Foncillas 2018) no PHB was detected at any time during the cultivation.

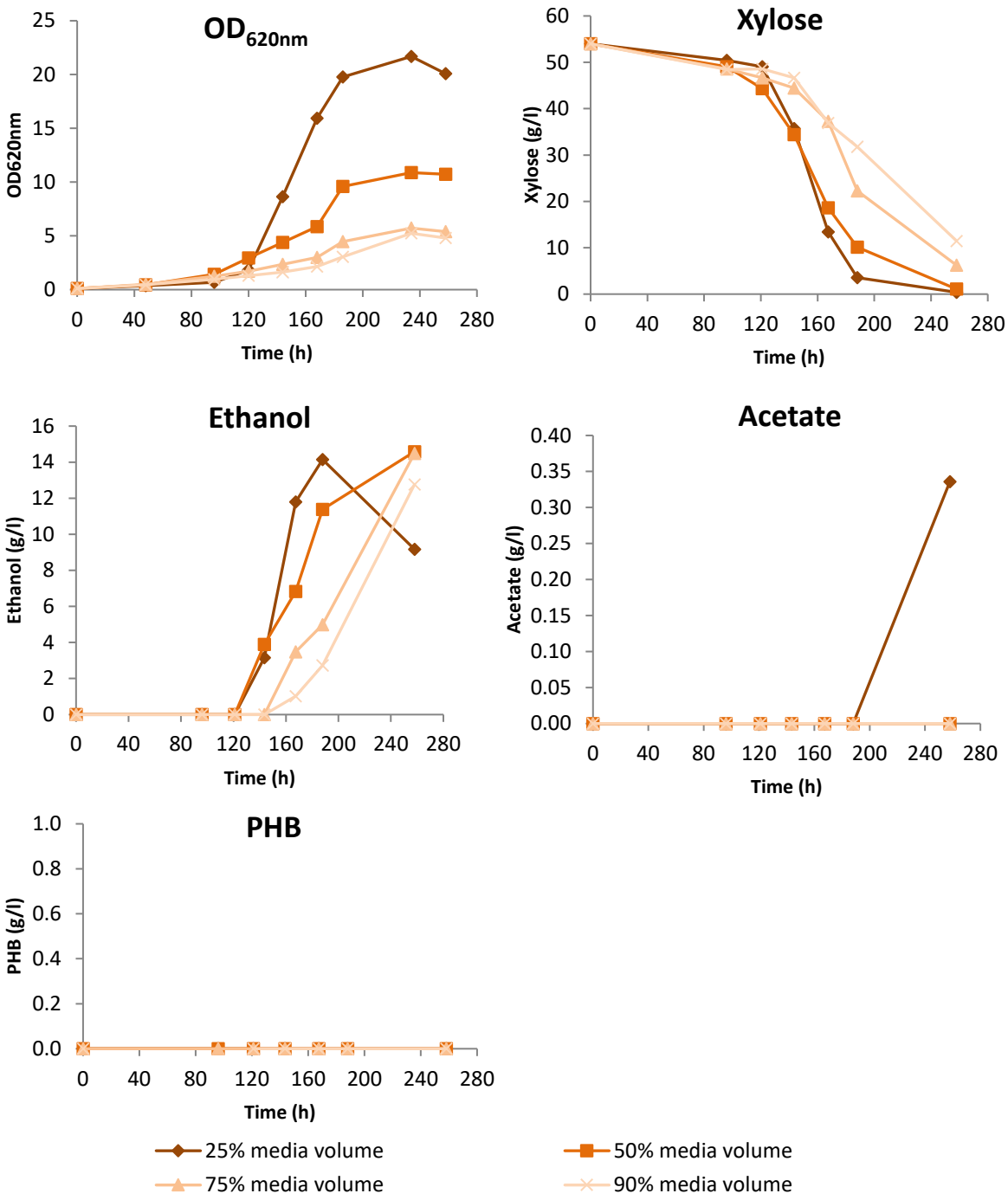

Figure 13. Effect of aeration on xylose consumption and product formation in the double deletion strain TMB4805 (XR/XDH, PHB, Acat rat, Δ*adh1*, Δ*ald6*). To obtain different aeration levels, a 250 ml shake flask was filled with different levels of growth medium and mixed with a magnetic stirrer. The percentages correspond to added media volume; 25%: 62.5 ml, 50%: 125 ml, 75%: 187.5 ml and 90%: 225 ml. Cultivations were performed in singlet.

3.2.3 Aldehyde dehydrogenase (ALD) activity assay

Enzyme activity assay was performed on the *ALD6* deleted strains along with positive and negative controls for further confirmation of the *ALD6* deletion. The increase in absorbance at 340 nm due to formation of NADPH was measured for 10 minutes at 30 °C. The results showed that no increase in absorbance could be detected not even in the positive control indicating that

the assay was not working. Due to time limitations the assay could not be further optimized and therefore neither reliable results nor conclusions were obtained.

3.3 Investigation of the effect of heterologous expression of the acetylating acetaldehyde dehydrogenase EutE on PHB production

From gathered data, it was found that no derivatives from TMB4495 or TMB4498 were able to produce PHB, which raised the question of whether the EutE enzyme was an interesting alternative for increasing PHB production. The EutE reaction may still go in the reverse direction (towards acetaldehyde) despite deletion of *ADH1* and *ALD6* genes. Other possibilities are that the *eutE* gene is not getting enough NAD^+ for efficient conversion or that the gene introduction somehow interferes with the PHB pathway. To investigate why the introduction of *eutE* abolishes PHB formation, the *eutE* gene was introduced again into the PHB producing strains TMB4800 (XR/XDH, PHB, Acat1rat) and TMB4803 (XR/XDH, PHB, Acat1rat Δ*ald6*). The CRISPR-Cas9 system was used to integrate the *eutE* cassette, where the gene was inserted on chromosome XII-5. One primer set was used for verification, allowing amplification of the inserted gene resulting in product size of 1471 bp.

Figure 14 shows PCR-verification of insertion of *eutE* in strains TMB4800 and TMB4803. In all three selected clones, a PCR product of the correct size was detected (Fig. 14 panel A). The clones that showed the strongest bands for each strain were run again in 0.8% agarose gel along with a negative (TMB4809) and a positive (TMB4810) control (Fig. 14 panel B).

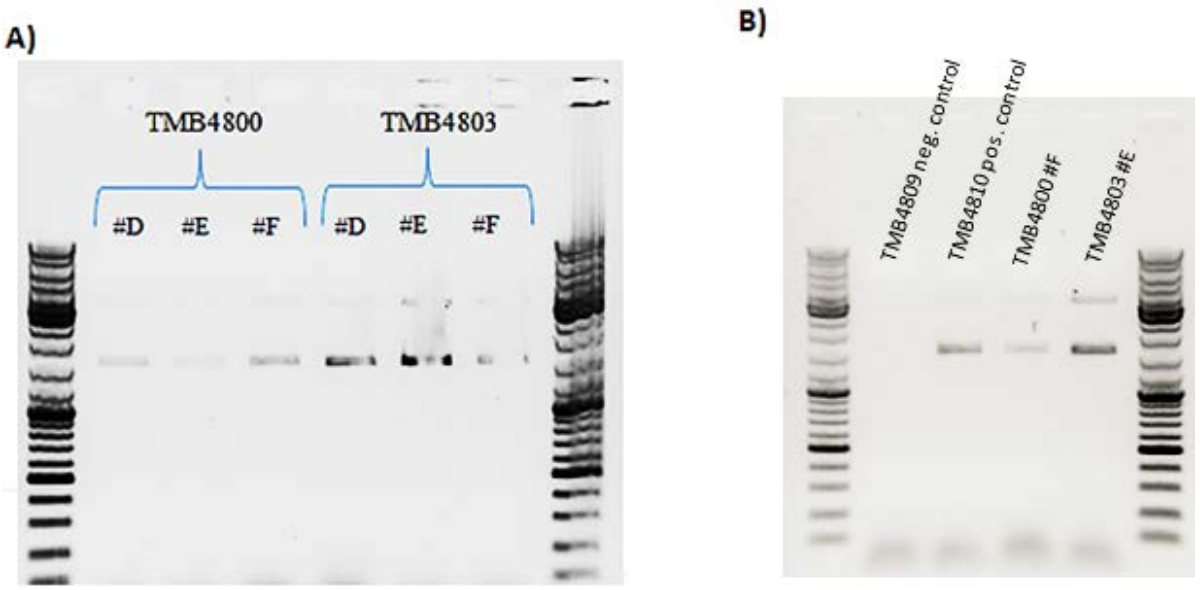

Figure 14. Verification of correct integration of the *eutE* gene in transformed yeast strains. A) from right: 1: ladder, 2: TMB4800 #D, 3: TMB4800 #E, 4: TMB4800 #F, 5: TMB4803 #D, 6: TMB4803 #E, 7 4803 #F, 8: ladder. B) from right: 1: ladder, 2: TMB4809 negative control, 3: TMB4819 positive control, 4: TMB4800 #F, 5: TMB4803 #E, 6: ladder. One primer set was used to verify the correct integration of the *eutE* gene in the *eutE* ORF and therefore only give a product if the gene is present.

An opposite approach was carried out in parallel where *eutE* was deleted in strains carrying the gene to see whether PHB production could be restored after removal. Experiments were carried out to delete *eutE* in strains TMB4495 and TMB4498 and replacing it with the marker amdSYM. The amSYM marker was amplified from pUG-amdSYM using primers containing homology to the *eutE* promoter and terminator. Clones were verified with colony-PCR where three PCR reactions were prepared using three different primer sets for verification. PCR1 to verify 5‘ integration of the amdSYM deletion cassette (451 bp) and PCR2 to verify 3‘ integration (462 bp). PCR3 amplifies a region of 1471 bp inside the *eutE* gene and should not give a product if the gene has been deleted. The amplified PCR reactions were then run on a 0.8% agarose gel. The correct *eutE* deletion was achieved only in one clone, TMB4498 clone D, since a PCR product was obtained in PCR1 and 2 but not in PCR3 as indicated with red circle in Figure 15.

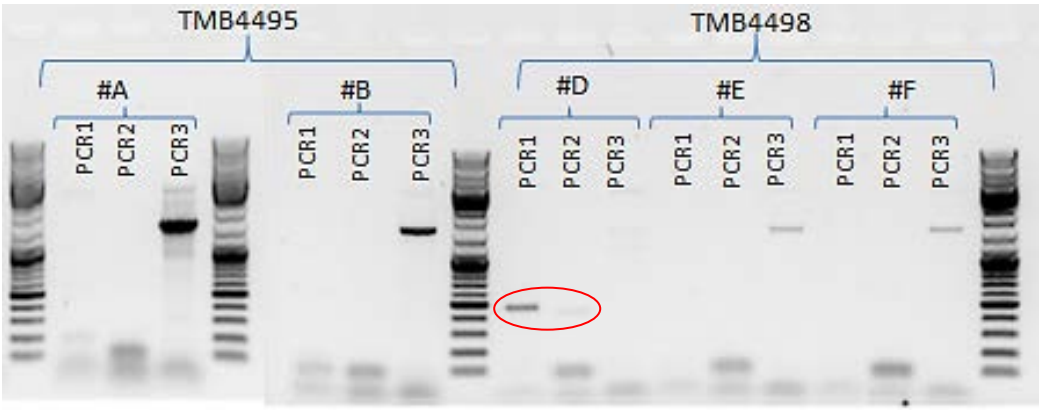

Figure 15. Verification of *eutE* deletion in TMB4495 and TMB4498. Two different primer sets were used to verify 5’ and 3’ integration of amdSYM, PCR1 (451 bp) and PCR2 (462 bp), respectively. Removal of the *eutE* gene was verified in PCR3 (1471 bp) that anneals internally in the *eutE* ORF and therefore only give a product if the gene is present. Correct verified clone is indicated with a red circle

3.3.1 Acetaldehyde CoA dehydrogenase activity assay

Enzyme activity assay was performed for further confirmation on both *eutE* deletion and *eutE* insertion in transformed strains as well as negative and positive controls. The EutE enzyme activity was calculated by monitoring the increase in absorbance at 340 nm due to formation of NADH and comparing that to an external standard curve. The obtained specific activity for each strain is listed in Table 7. The assay confirmed that TMB4803 clone #E had successfully been transformed and was expressing the EutE and the *eutE* had successfully been deleted in TMB4498 clone #D.

Table 7. EutE specific activity in following strains is listed in the table where the activity was calculated from undiluted samples.

Strain	Specific activity (µmol/min*mg)
	Undiluted
Blank	0.000 ± 0.000
TMB4425	(-) 0.003 ± 0.006
TMB4809	(-) 0.012 ± 0.007
TMB4495 (EutE)	0.038 ± 0.015
TMB4498 (EutE)	0.130 ± 0.006
TMB4801 (EutE)	0.069 ± 0.001
TMB4804 (EutE)[1]	0.070
TMB4805 (EutE)	0.224 ± 0.008
TMB4810 (EutE)	0.063 ±0.003
TMB4811 (EutE)	0.153 ± 0.000
TMB4813 (EutE)	0.114 ± 0.011
TMB4803+EutE #E	0.070 ± 0.006
TMB4498Δ*eutE* #B	0.105 ± 0.002
TMB4498Δ*eutE* #D	(-) 0.008 ± 0.025

[1] Specific activity for TMB4804 was calculated in singlet since one of that replicate showed no activity.

3.3.2 Aerobic cultivation of strains where *eutE* had been introduced or deleted to evaluate the effect on PHB formation

Correctly verified clones, TMB4803+EutE clone #E and TMB4498 Δ*eutE* clone #D, were cultivated along with the control strains TMB4425 and TMB4498 under aerobic conditions in YNB-xylose. The results including OD, xylose consumption and metabolite formation are presented in Figure 16. One replicate was done for each strain except for TMB4803+EutE, which was done in duplicate. For comparison, the yields were calculated for TMB4425, TMB4803+EutE, TMB4498 and TMB4498 Δ*eutE* and are listed in Appendix I (Table 9).

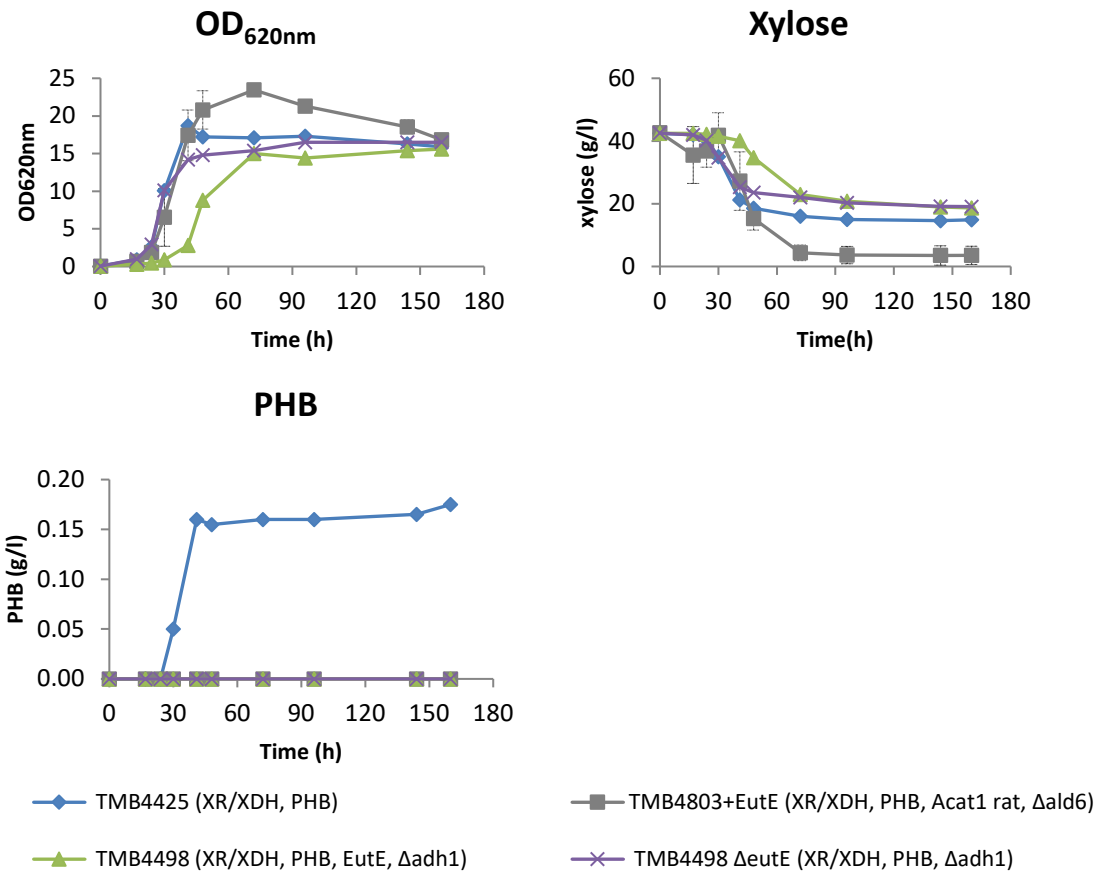

Figure 16. Xylose consumption and product formation of TMB4425, TMB4803+EutE, TMB4498 and TMB4498 Δ*eutE* under aerobic condition. The strains were cultivated in singlet except for TMB4803+EutE which was cultivated in biological duplicates in YNB-xylose. Values for TMB4803+EutE represent the average of the two replicates and the error bars correspond to the standard deviation.

The results in Figure 16 show that removal of *eutE* did not restore PHB production while integration of *eutE* in TMB4803 abolished PHB formation. These results together suggests that the effect of EutE must be on the genetic level of either one or several of the PHB genes *phaA*, *phaB* and/or *phaC*.

4. Discussion

One of the goals of this study was to see if the overexpression of homologs to the acetyl-CoA acetyltransferase PhaA encoded by *Acat1* and *ERG10* would enable PHB production in EutE strains. We hypothesised that in these strains, the EutE reaction was running in the reverse direction converting acetyl-CoA to acetaldehyde and thereby taking away the acetyl-CoA from the PHB pathway. Since both Acat1 and Erg10p have higher affinity for acetyl-CoA than *phaA* the idea was that these enzymes would more efficiently compete with EutE for the acetyl-CoA and thereby force the EutE reaction towards acetyl-CoA formation. However, the results from the fermentation experiments show that PHB could still not be produced in any of the strains carrying EutE and *Acat1* or *ERG10*. It was assumed that EutE was driving the reaction in the reverse direction that is, converting the acetyl-CoA back to acetaldehyde. This would thereby remove the substrate for the acetyl-CoA acetyltransferase enzymes and therefore no PHB will be produced. Therefore deletion of *ALD6* was carried out where the goal was to increase acetaldehyde availability to drive the EutE reaction towards acetyl-CoA formation and in that way also enable PHB formation in the EutE strains.

Deletion of *ALD6* should lead to increased ethanol formation in TMB4425 derived strains not carrying the *eutE* since there is no competition for the available acetaldehyde. However in the strains derived from TMB4495 and TMB4498 carrying *eutE*, there is an alternative route towards acetyl-CoA, which could compete with the alcohol dehydrogenase for the acetaldehyde resulting in acetyl-CoA production and PHB production (Fig. 17).

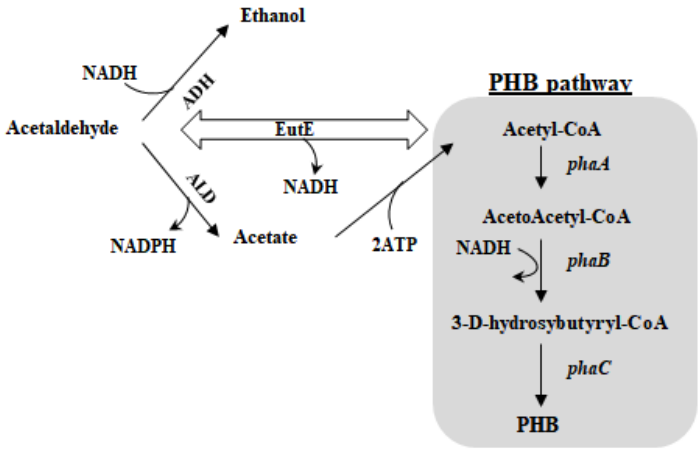

Figure 17. An overview of the metabolic flux from acetaldehyde in the PHB yeast strains when the *eutE* gene has been integrated.

The generated Δ*ald6* strains derived from TMB4495 carrying *eutE,* TMB4804 (TMB4801+Δ*ald6*) and TMB4813 (TMB4810+Δ*ald6*), showed no PHB production which was unexpected. Therefore it was hypothesised that EutE might have a negative effect on the PHB pathway, either on the genetic or on the protein level. The reaction might also only run in the reverse direction but this is not so likely since previous studies have shown that introduction

of EutE restores growth to wild type rate in an Ald$^-$ strain where all the five acetaldehyde dehydrogenases (*ALD*s) have been deleted (Kozak *et al.*, 2014). Since PHB was only produced in derived strains from TMB4425 (XR/XDH, PHB) and not in derived strains from TMB4495 (XR/XDH, PHB, EutE) and TMB4498 (XR/XDH, PHB, EutE, Δ*adh1*) carrying the *eutE* gene, concerns regarding the efficiency and functionality of EutE emerged. To elucidate this, an experiment was carried out to delete *eutE* in TMB4498 (XR/XDH, PHB, EutE,Δ*adh1*). This did not restore PHB production showing that the negative impact of EutE persist also once the protein was not active. In line with this, introduction of *eutE* in the PHB-producing strain TMB4803 (XR/XDH, PHB, Acat1opt, Δ*ald6*) completely abolished PHB production. These results together indicated that the effect of EutE could be on the genetic level, with an interaction with either one or several of the PHB genes *phaA, phaB* or *phaC*. One explanation could be that the *eutE* gene integrated on another chromosome, possibly on chromosome III where the PHB pathway is integrated in the *LEU2* locus, which could result in interference when the *pha* genes expression. The integration of *eutE* on chromosome XII-5 was done using primers containing 50 bp homology sequence to this specific integration site. However, if the *LEU2* locus on chromosome III where the PHB pathway is integrated has a similarity to the loci where the *eutE* should be integrated, a chance of incorrect integration could have occurred. To investigate this, the two 50 bp homology sequences were BLASTed against the *S. cerevisiae* CEN-PK 113-7D genome which resulted in only one match in the whole genome. This should illustrate that it is unlikely that the *eutE* would be integrated in another chromosome. Enzymatic activity assay were also performed for the acetoacetyl-CoA reductase (AAR) encoded by *phaB* but the assay was not successful and therefore no further conclusions could be drawn.

One interesting feature with the Δ*ald6* strains was that all, except for TMB4803, had an improved xylose consumption rate. The percentage of xylose consumed was 58 % for TMB4803, while TMB4804, TMB4812 and TMB4813 consumed over 92 % of the added xylose. This xylose consumption is superior to previously observed consumption for PHB strains carrying *ALD6* (Appendix I, Table 8 and 9). One explanation of the increased xylose consumption in the Δ*ald6* deleted strains could be that the oxido-reductase enzyme Zwf1, which is a component enzyme of the pentose phosphate pathway (PPP) got upregulated to maintain the levels of NADPH within the cells. It has been shown in previous studies that *S. cerevisiae* can upregulate Zwf1 as a stress response to maintain the redox state of the cells and thereby increase the flux in the PPP which enhances xylose utilization (Nobel *et al.* 2001). Furthermore, higher biomass formation was observed in the Δ*ald6* deleted strains which strengthens this assumption since the cells requires NADPH for biomass formation.

When comparing the maximum acetate formation in the strains where *ALD6* had been deleted, the Acat1 strains, TMB4803 and TBM4812 gave a yield of 0.20 ± 0.19 g acetate/g xylose and 0.16 ± 0.04 g acetate/g xylose while the Erg10p strains, TMB4804 and TMB4813 gave yield of 0.10 ± 0.03 g acetate/g xylose and TMB4813 0.15 ± 0.01 g acetate/g xylose. The Δ*ald6* strains still produced acetate but in lower concentrations compared to the yeast strains still carrying the *ALD6* gene. This was expected since the cells can upregulate other acetaldehyde dehydrogenase and therefore the acetate formation will not abort completely (Luo *et al.* 2013). Furthermore, strains carrying the *eutE*, TMB4804 and TMB4813 showed higher ethanol titer

(8.23 ± 0.37 g/l and 6.14 ± 0.38 g/l) than strains TMB4803 and TMB4812, lacking the *eutE* (2.97 ± 2.31 g/l and 6.00 ± 0.01 g/l). This was unexpected since EutE should catalyse the conversion of acetaldehyde to acetyl-CoA and thereby decrease the ethanol formation. This could be due to the high efficiency of the alcohol dehydrogenases catalysing the ethanol synthesis and using up the acetaldehyde pool and therefore forcing EutE to drive the reaction back from acetyl-CoA in the reverse direction to acetaldehyde.

It is also worth to mention that weak correlation was obtained between the two replicates for TMB4803 when comparing substrate consumption and metabolite formation. Therefore one replicate should be repeated, but due to time limitation it was not possible to include in the current study.

5. Conclusions

In the present study, only strains derived from TMB4425 were able to produce PHB, whereas all strains containing EutE integration did not. Due to this, it was not possible to conclude whether the Acat1 and Erg10p would positively impact PHB production in the presence of EutE. As deletion of EutE did not restore PHB production, the integration site of EutE and its effect on the PHB genes must be reassessed, for instance by performing DNA sequencing of the involved regions in order to understand why EutE integration silenced one or several of the PHB genes.

6. References

Carlson, R. and Srienc, F. (2006). Effects of recombinant precursor pathway variations on poly[(*R*)-3-hydroxybutyrate] synthesis in *Saccharomyces cerevisiae*. *Journal of Biotechnology 124*(3): 561-573.

de las Heras A. M. (2017). Application of synthetic biology for biopolymer production using *Saccharomyces cerevisiae.* Media-Tryck: Lund University.

de las Heras, A. M., Portugal-Nunes, D. J., Rizza, N., Sandström, A. G. and Gorwa-Grauslund, M. F. (2016-a). Anaerobic poly-3-D-hydroxybutyrate production form xylose in recombinant *Saccharomyces cerevisiae* using a NADH-dependant acetoacetyl-CoA reductase. *Microb Cell Fact 15*: 197.

de las Heras, A. M., Bjurman, N., Landberg, J. And Gorwa-Grauslund, M. F. (2016-b). Rewiring the central carbon metabolism for poly-3-D-hydroxybutyrate production in *Saccharomyces cerevisiae.* Lund University.

du Preez, J. C. and Prior, B. A. (1985). A quantitative screening of some xylose-fermenting yeast isolates. *Biotechnol Lett 7*(4): 241-246.

Gietz, R. D. and Schiestl, R. H. (2007) High-efficiency yeast transformation using the LiAc/SS carrier DNA/PEG method. *Nature Protocols, 2*(1): 31-34.

Gironi, F. and Piemonte, V. (2011). Bioplastics and patroleum-based plastics: Strengths and weaknesses. *Energ Sourc 33*:1949-1959.

Gupta, R. M. and Musunuru, K. (2014). Expanding the genetic editing tool kit: ZFNs, TALENs, and CRISPR-Cas9. *J Clin Invest 124*(10): 4154-4161.

Hiser, L., Basson, M. E. and Rine, J. (1994). ERG10 from *Saccharomyces cerevisiae* encodes acetoacetyl-CoA thiolase. *Journal of Biological Chemistry, 269*(50): 31383-31389.

Hou, J., Qiu, C., Shen, Y., Li, H. and Bao, X. (2017). Engineering of *Saccharomyces cerevisiae* for the efficient co-utilization of glucose and xylose. *FEMS Yeast Research, 17*(4).

Hsu, P. D., Lander, E. S. and Zhang, F. (2014). Development and applications of CRISPR-Cas9 for genome engineering. *Cell 157*(6): 1262-1278.

Jeffries, T. W. (1983). Utilization of xylose by bacteria, yeasts, and fungi. *Adv Biochem Eng Biotechnol 27*: 1-32.

Jessop-Fabre, M. M., Jakočiūnas, T., Stovicek, V., Dai, Z, Jensen, M. K., Keasling, J. D. and Borodina, I. (2016). EasyClone-MarkerFree: A vector toolkit for marker-less integration of genes into *Saccharomyces cerevisiae* via CRISPR-Cas9. *Biotechnol J. 11*(8): 1110-1117.

Kozak, B. U., van Rossum, H. M., Benjamin, K. R., Wu, L., Daran, J-M. G., Pronk, J. T. and

van Maris, A. J. A. (2014). Replacement of the *Saccharomyces cerevisiae* acetyl-CoA synthetases by alternative pathways for cytosolic acetyl-CoA synthesis. *Metabolic Engineering 21*: 46-59.

Law, J. H. and Slepecky, R. A. (1961). Assay of poly-beta-hydroxybutyric acid. *J Bacteriol 83*: 33-36.

Lee, S. Y. (1996). Plastic bacteria? Progress and prospects for polyhydroxyalkanoate production in bacteria. *Trends in biotechnology 14*(11): 431-438.

Luo, Z., Walkey, C. J., Madilao, L. L., Measday, V. and Van Vuuren, H. J. J. (2013). Functional improvement of *Saccharomyces cerevisiae* to reduce volatile acidity in wine. *FEMS yeast research 13*(5): 485-494.

Medina, V. G., Almering, M. J. H., van Maris, A. J. A. and Pronk, T. (2010). Elimination of glycerol production in anaerobic cultures of a *Saccharomyces cervisiae* strain engineered to use acetic acid as an electron acceptor. *Appl Environ Microbiol. 76*(1): 190-195.

Middleton, B. (1974). The kinetic mechanism and properties of the cytoplasmic acetoacetyl-coenzyme A thiolase from rat liver. *Biochem. J. 139*(1): 109-121.

Moysés, D. N., Reis, V. C. B., de Almeida, J. R. M., de Moraes, L. M. P., and Torres, F. A. G. (2016). Xylose Fermentation by *Saccharomyces cerevisiae*: Challenges and Prospects. *International Journal of Molecular Sciences*, *17*(3): 207.

Nobel, de H., Lawrie, L., Brul, S., Klis, F., Davis, M., Alloush, H. and Coote, P. (2001). Parallel and comparative analysis of the proteome and transcriptome of sorbic acid-stressed *Saccharomyces cerevisiae*. *Yeast 18*: 1413-1428.

Perruca Foncillas (2018). Metabolic engineering of *Saccharomyces cerevisiae* for improving PHB production. Advanced course report. [Unpublished].

Saint-Prix F., Bönquist, L. and Dequin, S. (2004). Functional analysis of the ALD gene family of *Saccharomyces cerevisiae* during anaerobic growth on glucose: the NADP+-dependent Ald6p and Ald5p isoforms play a major role in acetate formation. *Microbiology 150*(7): 2209-20.

Sandström, A. G., de las Heras, A. M., Portugal-Nunes, D. and Gorwa-Grauslund, M. F. (2015). Engineering of *Saccharomyces cerevisiae* for the production of poly-3-D-hydroxybutyrate from xylose. *AMB Express 5*: 14.

Solis-Escalante, D., Kuijpers, N. G., Nadine, B., Bolat, I., Bosman, L., Pronk, J. T., Daran, J-M. and Daran-Lapujade, P. (2013). amdSYM, a new dominant recyclable marker cassette for *Saccharomyces cerevisiae*. *FEMS Yeast Res* 13:126-139.

Wang, P. Y. and Schneider, H. (1980). Growth of yeasts on D-xylulose *Canadian Journal of Microbiology, 26*(9): 1165-1168.

Young, S. AM., Aitken, J. R. and Ikawa, M. (2015). Advantages of using the CRISPR/Cas9 system of genome editing to investigate male reproductive mechanisms using mouse models. *Asian J Androl 17*(4): 623-627.

Yun, E. J.,, Kwak, S., Kim, S. R., Park, Y. C., Jin, Y. S. and Kim, K. H. (2015). Production of (*S*)-3-hydroxybutyrate by metabolically engineered *Saccharomyces cerevisiae*. *Journal of Biotechnology 209*: 23-30.

Appendix I – Yield calculations

Table 8. Calculated yields for cultivations of reference strains TMB4425, TMB4495 and TMB4498 under aerobic conditions performed in another study (Perruca Foncillas 2018). The values represent average values of the duplicates as well as standard deviation.

Strain	**TMB4425** NADH-PHB; Xrmut	**TMB4495** NADH-PHB; Xrmut; EutE;	**TMB4498** NADH-PHB; Xrmut; EutE; Δ*adh1*
Cultivation time (h)	160 h	160 h	160 h
Flask and media vol.	SF 1L-0.1L media 50 g/l xylose	SF 1L-0.1L media 50 g/l xylose	SF 1L-0.1L media 50 g/l xylose
Growth condition	Shake flask (Aerobic)	Shake flask (Aerobic)	Shake flask (Aerobic)
Biomass (g/l)	3.81 ± 0.18	3.74 ± 0.26	3.64 ± 0.16
Growth rate (h^{-1})	0.15 ± 0.01	0.14 ± 0.00	0.15 ± 0.00
Ysx (g/g Xyl)	0.13 ± 0.01	0.13 ± 0.01	0.14 ± 0.00
YsEtOH (g/g Xyl)*	0.12 ± 0.02	0.10 ± 0.01	0.07 ± 0.01
YsAc (g/g Xyl)*	0.22 ± 0.03	0.24 ± 0.01	0.26 ± 0.02
YsXylitol (g/g Xyl)	0.05 ± 0.01	0.08 ± 0.00	0.07 ± 0.00
YsGly (g/g Xyl)	0.02 ± 0.00	0.02 ± 0.00	0.02 ± 0.00
Ethanol titer (g/L)	3.03 ± 0.93	2.35 ± 0.23	1.27 ± 0.08
YsPHB (mg PHB/g Xyl)	8.4 ± 0.43	0.00 ± 0.00	0.00 ± 0.00
PHB titer (g/L)	0.25 ± 0.04	0.00 ± 0.00	0.00 ± 0.00
Xylose/sugar consumed (%)	56.18 ± 6.35	53.66 ± 0.22	48.61 ± 1.77
Reference	Perruca Foncillas (2018)	Perruca Foncillas (2018)	Perruca Foncillas (2018)

* Yields were calculated using the maximum metabolite values.

Table 9. An overview of calculated yields for all cultivated strains in current study. The values represent average values of the duplicates as well as standard deviation except for strains TMB4425, TMB4498 and TMB4498Δ*ald6*.

Strain	TMB4800 NADH-PHB; Xrmut; Acat1 rat	TMB4801 NADH-PHB; Xrmut; EutE; Acat1 rat	TMB4802 NADH-PHB; Xrmut; EutE; Δ*adh1*; Acat rat	TMB4803 NADH-PHB; Xrmut; Acat1 rat; Δ*ald6*	TMB4804 NADH-PHB; Xrmut; EutE; Acat1 rat; Δ*ald6*	TMB4809 NADH-PHB; Xrmut; 3xErg10p	TMB4810 NADH-PHB; Xrmut; EutE; 3xErg10p	TMB4811 NADH-PHB; Xrmut; EutE; Δ*adh1*; 3xErg10p	TMB4812 NADH-PHB; Xrmut; 3xErg10p; Δ*ald6*	TMB4813 NADH-PHB; Xrmut; EutE; 3xErg10p; Δ*ald6*	TMB4425 NADH-PHB; XRmut	TMB4803 +EutE NADH-PHB; Xrmut; Acat1 rat; Δ*ald6*	TMB4498 NADH-PHB; Xrmut; *eutE;* Δ*adh1*	TMB4498 Δ*eutE* NADH-PHB; Xrmut; Δ*eutE;* Δ*adh1*
Cultivation time (h)	160 h	160 h	160 h	160 h	160 h	160 h	160 h	160 h	160 h	160 h	160 h	160 h	160 h	160 h
Flask and media vol.	SF 1L-0.1L media 50 g/l xylose Shake flask	SF 1L-0.1L media 50 g/l xylose Shake flask	SF 1L-0.1L media 50 g/l xylose Shake flask	SF 1L-0.1L media 50 g/l xylose Shake flask	SF 1L-0.1L media 50 g/l xylose Shake flask	SF 1L-0.1L media 50 g/l xylose Shake flask	SF 1L-0.1L media 50 g/l xylose Shake flask	SF 1L-0.1L media 50 g/l xylose Shake flask	SF 1L-0.1L media 50 g/l xylose Shake flask	SF 1L-0.1L media 50 g/l xylose Shake flask	SF 1L-0.1L media 50 g/l xylose Shake flask	SF 1L-0.1L media 50 g/l xylose Shake flask	SF 1L-0.1L media 50 g/l xylose Shake flask	SF 1L-0.1L media 50 g/l xylose Shake flask
Growth condition	(Aerobic)	(Aerobic)	(Aerobic)	(Aerobic)	(Aerobic)	(Aerobic)	(Aerobic)	(Aerobic)	(Aerobic)	(Aerobic)	(Aerobic)	(Aerobic)	(Aerobic)	(Aerobic)
Biomass (g/l)	3.64 ± 0.05	3.95 ± 0.66	3.90 ± 0.92	4.92 ± 1.29	5.49 ± 0.17	3.46 ± 0.04	3.78 ± 0.07	3.77 ± 0.52	4.62 ± 0.21	4.56 ± 0.29	3.48	4.12 ± 0.08	4.37	4.17
Growth rate (h^{-1})	0.16 ± 0.00	0.15 ± 0.00	0.13 ± 0.00	0.13 ± 0.02	0.14 ± 0.02	0.12 ± 0.01	0.11 ± 0.01	0.12 ±0.01	0.12 ± 0.01	0.11 ± 0.00	0.13	0.14 ± 0.01	0.11	0.11
Ysx (g/g Xyl)	0.13 ± 0.00	0.12 ± 0.01	0.16 ± 0.02	0.19 ± 0.09	0.12 ± 0.00	0.12 ± 0.00	0.12 ± 0.01	0.14 ± 0.02	0.12 ± 0.01	0.11 ± 0.01	0.13	0.11 ± 0.01	0.18	0.18
YsEtOH (g/g Xyl)*	0.12 ± 0.01	0.13 ± 0.00	0.04 ± 0.03	0.09 ± 0.04	0.19 ± 0.02	0.14 ± 0.01	0.13 ± 0.03	0.07 ± 0.03	0.17 ± 0.01	0.17 ± 0.01	0.11	0.17 ± 0.01	0	0.04
YsAc (g/g Xyl)*	0.23 ± 0.02	0.20 ± 0.01	0.25 ± 0.05	0.20 ± 0.19	0.10 ± 0.03	0.21 ± 0.04	0.15 ± 0.14	0.23 ± 0.02	0.14 ± 0.01	0.14 ± 0.00	0.24	0.08 ± 0.04	0.24	0.26
YsXylitol (g/g Xyl)	0.05 ± 0.00	0.07 ± 0.02	0.06 ± 0.01	0.04 ± 0.04	0.01 ± 0.00	0.04 ± 0.02	0.07 ± 0.03	0.07 ± 0.01	0.01 ± 0.00	0.01 ± 0.00	0.045	0.01 ± 0.00	0.04	0.07
YsGly (g/g Xyl)	0.02 ± 0.01	0.03 ± 0.02	0.03 ± 0.01	0.07 ± 0.03	0.03 ± 0.01	0.03 ± 0.00	0.02 ± 0.00	0.03 ± 0.01	0.04 ± 0.01	0.02 ± 0.00	0.02	0.03 ± 0.00	0.03	0.03
Ethanol titer (g/L)*	2.78 ± 0.22	3.33 ± 0.17	0.68 ± 0.58	2.97 ± 2.31	8.23 ± 0.37	3.22 ± 0.73	3.67 ± 0.37	1.59 ± 0.85	6.00 ± 0.01	6.14 ± 0.38	2.25	5.89 ± 0.90	0.04	0.69
YsPHB (mg PHB /g Xyl)	9.62 ± 1.50	0.00 ± 0.00	0.00 ± 0.00	6.09 ± 1.74	0.00 ± 0.00	8.62 ± 1.14	0.00 ± 0.00	0.00 ± 0.00	6.09 ± 0.09	0.00 ± 0.00	6.35	0.00 ± 0.00	0.00 ± 0.00	0.00 ± 0.00

PHB titer (g/L)	0.27 ± 0.05	0.00 ± 0.00	0.00 ± 0.00	0.17 ± 0.07	0.00 ± 0.00	0.25 ± 0.04	0.00 ± 0.00	0.00 ± 0.00	0.24 ± 0.00	0.00 ± 0.00	0.18	0.00 ± 0.00	0.00 ± 0.00	0.00 ± 0.00
Xylose/sugar consumed (%)	53.11 ± 1.4	62.79 ± 5.97	46.54 ± 3.7	57.71 ± 39.69	92.59 ± 3.73	65.62 ± 0.21	69.76 ± 6.98	58.78 ± 0.72	92.33 ±0.15	93.64 ± 1.2	64.94	91.65 ± 7.29	56.06	55.12
Reference	Perruca Foncillas (2018)	Perruca Foncillas (2018)	Perruca Foncillas (2018)	Perruca Foncillas (2018) & this study	Perruca Foncillas (2018) & this study	This study	This study	This study	This study	This study	This study	This study	This study	This study

[*] Yields were calculated using the maximum metabolite values.

Table 10. Calculated yields for cultivations of TMB4805 under different conditions.

Strain	**TMB4805** NADH-PHB; Xrmut; EutE; Δ*adh1*; Acat1 rat; Δ*ald6*	**TMB4805** NADH-PHB; Xrmut; EutE; Δ*adh1*; Acat1 rat; Δ*ald6*	**TMB4805** NADH-PHB; Xrmut; EutE; Δ*adh1*; Acat1 rat; Δ*ald6*	**TMB4805** NADH-PHB; Xrmut; EutE; Δ*adh1*; Acat1 rat; Δ*ald6*	**TMB4805** NADH-PHB; Xrmut; EutE; Δ*adh1*; Acat1 rat; Δ*ald6*	**TMB4805** NADH-PHB; Xrmut; EutE; Δ*adh1*; Acat1 rat; Δ*ald6*
Cultivation time (h)	160 h	160 h	258 h	258 h	258 h	258 h
Flask and media vol.	SF 1L-0.1L media 20 g/l glucose	SF 1L-0.1L media 20 g/l glucose/xylose	SF 250mL-62.5ml 50 g/l xylose	SF 250mL-125ml 50 g/l xylose	SF 250mL-187.5ml 50 g/l xylose	SF 250mL-225ml 50 g/l xylose
Growth condition	Shake flask (Aerobic)	Shake flask (Aerobic)	Waterbath w/magnet	Waterbath w/magnet)	Waterbath w/magnet	Waterbath w/magnet
Biomass (g/l)	1.96 ± 0.71	5.17 ± 1.35	6.53	3.97	2.39	2.27
Growth rate (h^{-1})	0.08 ± 0.01	0.07 ± 0.01	0.05	0.02	0.01	0.01
Ysx (g/g Xyl)	0.09 ± 0.03	-	0.12	0.07	0.05	0.05
YsEtOH (g/g Xyl)[1]	0.22 ± 0.06	0.25 ± 0.01[2]	0.28	0.28	0.30	0.30
YsAc (g/g Xyl)[1]	0.00 ± 0.00	0.12 ±0.06[3]	0.01	0.00	0.00	0.00
YsXylitol (g/g Xyl)	0.00 ± 0.00	0.02 ± 0.00[3]	0.07	0.12	0.16	0.15
YsGly (g/g Xyl)	0.32 ± 0.00	0.27 ± 0.03[2]	0.03	0.06	0.11	0.11
Ethanol titer (g/L)	4.83 ± 1.29	5.18 ± 0.29	14.14	14.58	14.49	12.76
YsPHB (mg PHB/g Xyl)	0.00 ± 0.00	0.00 ± 0.00	0.00	0.00	0.00	0.00
PHB titer (g/L)	0.00 ± 0.00	0.00 ± 0.00	0.00	0.00	0.00	0.00
Xylose (glucose)/sugar consumed (%)	(100.00 ± 0.00)	72.33 ± 7.51 (100.00 ± 0.00)	99.27	98.01	88.48	78.76
Reference	This study	This study	This study	This study	This study	This study

[1] Yields were calculated using the maximum metabolite values. [2] Yields were calculated as g/g glucose. [3]Yields were calculated as g/g xylose.